研 究 成 果 の 刊 行 に 関 す る 一 覧 表

原著論文

著者	論文タイトル	掲載誌名	巻 ページ	出版年
Miyazaki K, Fujita T, Ozaki T, Kato C, Kurose Y, Sakamoto M, Kato S, Goto T, Itoyama Y, Aoki M, Nakagawara A	NEDL1, a novel ubiquitin-protein isopeptide ligase for dishevelled-1, targets mutant superoxide dismutase-1	J Biol Chem	279 11327-11335	2004
Kato S, Saeki Y, Aoki M, Nagai M, Ishigaki A, Itoyama Y, Kato M, Asayama K, Awaya A, Hirano A, Ohama E	Histological evidence of redox system breakdown caused by superoxide dismutase 1 (SOD1) aggregation is common to SOD1-mutated motor neurons in humans and animal models	Acta Neuropathol	107 149-158	2004
Yasuda H, Ebihara S, Yamaya M, Asada M, Sasaki H, Aoki M	Increased arterial carboxyhaemoglobin concentrations in patients with sporadic amyotrophic lateral sclerosis	J Neurol Neurosurg Psychiatry	75 1076-1077	2004
Suzuki N, Aoki M, Takahashi T, Takano D, Asano M, Shiga Y, Onodera Y, Tateyama M, Itoyama Y	Novel dysferlin mutations and characteristic muscle atrophy in late-onset Miyoshi myopathy	Muscle Nerve	29 721-723	2004
Nagashima T, Chuma T, Mano Y, Goto Y, Hayashi YK, Minami N, Nishino I, Nonaka I, Takahashi T, Sawa H, Aoki M, Nagashima K	Dysferlinopathy associated with rigid spine syndrome	Neuropath	24 341-6	2004
Suzuki N, Aoki M, Hinuma Y, Takahashi T, Onodera Y, Ishigaki A, Kato M, Warita H, Tateyama M, Itoyama Y	Expression profiling with progression of dystrophic change in dysferlin-deficient mice (SJL)	Neurosci Res	in press	
Fujiwara N., Miyamoto Y., Ogasahara K., Takahashi M., Ikegami T., Takamiya R., Suzuki K. and Taniguchi N.	Different Immunoreactivity against Monoclonal Antibodies between Wild-type and Mutant Copper/Zinc Superoxide Dismutase Linked to Amyotrophic Lateral Sclerosis	J. Biol. Chem.	280 5061-5070	2005

著者	論文タイトル	掲載誌名	巻 ページ	出版年
Takamiya R., Takahashi M., Park Y.S. Tawara Y., Fujiwara N., Miyamoto Y., Gu J., Suzuki K. and Taniguchi N.	Overexpression of Mutated Cu,Zn-SOD in Neuroblastoma Cells Results in Cytoskeletal Change	Am. J. Physiol. Cell Physiol	288 C253-259	2005
Hanamoto T, Ozaki T, Furuya K, Hosoda M, Hayashi S, Nakanishi M, Yamamoto H, Kikuchi H, Todo S, Nakagawara A.	Identification of protein kinase A catalytic subunit _ (PKA-C_) as a novel binding partner of p73 and regulation of p73 function.	J. Biol. Chem.	in press	
Ohira M, Oba S, Nakamura Y, Hirata T, Ishii S, Nakagawara A.	A review of DNA microarray analysis of human neuroblastomas.	Cancer Lett.	in press	
Lin L, Ozaki T, Takada Y, Kageyama H, Nakamura Y, Hata A, Zhang J-H, Simonds W, Nakagawara A, Koseki H.	Topors, a p53 and topoisomerase I-binding RING finger protein, is a co-activator of p53 in growth suppression induced by DNA damage.	Oncogene	in press	
Ozaki T, Hosoda M, Miyazaki K, Hayashi S, Watanabe K, Nakagawa T, Nakagawara A.	Functional implication of p73 protein stability in neuronal cell survival and death..	Cancer Lett.	in press	
Kato C, Hanamoto T, Nakagawara A.	Protein stability and function of p73 are modulated by a physical interaction with RanBPM in mammalian cultured cells.	Oncogene	24 938-944	2005
Abe M, Ohira M, Kaneda A, Yagi Y, Yamamoto S, Kitano Y, Takato T, Nakagawara A, Ushijima T.	CpG island methylator phenotype is a strong determinant of poor prognosis in neuroblastomas.	Cancer Res.	65 828-834	2005
Nakagawara A, Ohira M.	Comprehensive genomics linking between neural development and cancer: Neuroblastoma as a model. In Special Issue: Neural development and cancer.	Cancer Lett.	204 23-224	2004
Miyazaki K, Fujita T, Ozaki T, Kato C, Kurose Y, Sakamoto M, Kato S, Goto T, Itoyama Y, Aoki M, Nakagawara A.	NEDL1, a novel ubiquitin-protein isopeptide ligase for Dishevelled-1, targets mutant superoxide dismutase-1.	J. Biol. Chem.	279 11327-11335	2004

著者	論文タイトル	掲載誌名	巻 ページ	出版年
Hamano S, Ohira M, Isogai E, Nakada K, Nakagawara A.	Identification of novel human neuronal leucine-rich repeat (hNLRR) family genes and inverse association of expression of Nbla10449/hNLRR-1 and Nbla10677/hNLRR-3 with the prognosis of primary neuroblastomas.	Int. J. Oncol.	24 1457-1466	2004
Ohtori S, Isogai E, Hasue F, Ozaki T, Nakamura Y, Nakagawara A, Koseki H, Yuasa S, Hanaoka E, Shinbo J, Yamamoto T, Chiba H, Yamazaki M, Moriya H, Sakiyama S.	Reduced inflammatory pain in mice deficient in the differential screening-selected gene abrrative in neuroblastoma.	Mol. Cell. Neurosci.	245 504-514	2004
K, Yu L, Ogi T, Takenaga K, Shishikura T, Nakagawara A, Sakiyama S, Tagawa M and O-Wang J.	Elevated expression of DNA polymerase k in human lung cancer is associated with p53 inactivation: negative regulation of POLK promoter activity by p53.	Int. J. Oncol.	25 161-165	2004
Ando K, Ozaki T, Yamamoto H, Furuya K, Hosoda M, Hayashi S, Fukuzawa M, Nakagawara A.	Polo-like kinase 1 (Plk1) inhibits p53 function by physical interaction and phosphorylation.	J. Biol. Chem.	279 25549-25561	2004
Hiyama E, Yamaoka H, Matsunaga T, Hayashi Y, Ando H, Suita S, Horie H, Kaneko M, Sasaki F, Hashizume K, Nakagawara A, Ohnuma N, Yokoyama T.	High expression of telomerase is an independent prognostic indicator of poor outcome in hepatoblastoma.	Br. J. Cancer	291 972-979	2004
Yamada S, Ohira M, Horie H, Ando K, Takayasu H, Suzuki Y, Sugano S, Matsunaga T, Hiyama E, Hayashi Y, Watanabe Y, Suita S, Kaneko M, Sasaki F, Hashizume K, Ohnuma N, Nakagawara A.	Expression profiling and differential screening between hepatoblastomas and the corresponding normal livers: Identification of high expression of the Plk1 oncogene as a poor-prognostic indicator of hepatoblastomas.	Oncogene	23 5901-5911	2004
Takahashi M, Ozaki T, Todo S, Nakagawara A.	Decreased expression of the candidate tumor suppressor gene ING1 is associated with poor prognosis in advanced neuroblastomas.	Oncol Rep.	12 811-816	2004

著者	論文タイトル	掲載誌名	巻 ページ	出版年
Kato C, Miyazaki K, Nakagawa A, Ohira M, Nakamura Y, Ozaki T, Imai T, Nakagawara A.	Low expression of human tubulin tyrosine ligase and suppressed tubulin tyrosination/detyrosination cycle are associated with impaired neuronal differentiation in neuroblastomas with poor prognosis.	Int. J. Cancer	112 365-375	2004
Isogawa K, Akiyoshi J, Kodama K, Matsushita H, Takahashi, Tsutsumi T, Funakoshi H, Nakamura T.	Anxiolytic effect of hepatocyte growth factor infused into rat brain.	Neuropsychobiology	51(1) 34-38	2004
Date I, Takagi N, Takagi K, Kago T, Matsumoto K, Nakamura T, Takeo S.	Hepatocyte growth factor attenuates cerebral ischemia-induced learning dysfunction.	Biochem Biophys Res Commun.	319(4) 1152-8	2004
Date I, Takagi N, Takagi K, Kago T, Matsumoto K, Nakamura T, Takeo S.	Hepatocyte growth factor improved learning and memory dysfunction of microsphere-embolized rats.	J Neurosci Res.	78(3) 442-5	2004
Oshima K, Shimamura M, Mizuno S, Tamai K, Doi K, Morishita R, Nakamura T, Kubo T, Kaneda Y.	Intrathecal injection of HVJ-E containing HGF gene to cerebrospinal fluid can prevent and ameliorate hearing impairment in rats.	FASEB J.	18(1) 212-4	2004

書　籍

著者	論文タイトル	書籍全体の編集者	書籍名	出版社	巻 ページ	出版年
青木正志	新世代の筋萎縮性側索硬化症（ALS）の動物モデル		細胞工学		23 838-841	2004
青木正志、永井真貴子、石垣あや、糸山泰人	神経栄養因子HGFの髄腔内投与によるALS治療法の開発		最新医学		59 87-93	2004
Nakagawara A.	Molecular and developmental biology of neuroblastoma	S. Cohn & N-K. Cheung	Neuroblastoma	Springer-Verlag, Heidelberg	in press	2005
Nakagawara A.	In NGF and Related Molecules in Health and Disease: Neural crest development and neuroblastoma: the genetic and biological link.	Luigi Aloe & Laura Calza	Progess in Brain Research	Elservier Science Publisher	146 233-242	2004

THE JOURNAL OF BIOLOGICAL CHEMISTRY
Vol. 279, No. 12, Issue of March 19, pp. 11327–11335, 2004
Printed in U.S.A.

NEDL1, a Novel Ubiquitin-protein Isopeptide Ligase for Dishevelled-1, Targets Mutant Superoxide Dismutase-1*

Received for publication, November 12, 2003, and in revised form, December 16, 2003
Published, JBC Papers in Press, December 18, 2003, DOI 10.1074/jbc.M312389200

Kou Miyazaki‡, Tomoyuki Fujita‡, Toshinori Ozaki‡, Chiaki Kato‡, Yuka Kurose‡, Maya Sakamoto‡, Shinsuke Kato§, Takeshi Goto¶, Yasuto Itoyama‖, Masashi Aoki‖, and Akira Nakagawara‡

From the ‡Division of Biochemistry, Chiba Cancer Center Research Institute, Chiba 260-8717, Japan, the §Division of Neuropathology, Institute of Neurological Sciences, Faculty of Medicine, Tottori University, Yonago 683-8504, Japan, ¶Hisamitsu Pharmaceutical Company Incorporated, Tokyo 100-622, Japan, and the ‖Department of Neurology, Tohoku University School of Medicine, Sendai 980-8574, Japan

Approximately 20% of familial amyotrophic lateral sclerosis (FALS) arises from germ-line mutations in the superoxide dismutase-1 (*SOD1*) gene. However, the molecular mechanisms underlying the process have been elusive. Here, we show that a neuronal homologous to E6AP carboxyl terminus (HECT)-type ubiquitin-protein isopeptide ligase (NEDL1) physically binds translocon-associated protein-δ and also binds and ubiquitinates mutant (but not wild-type) SOD1 proportionately to the disease severity caused by that particular mutant. Immunohistochemically, NEDL1 is present in the central region of the Lewy body-like hyaline inclusions in the spinal cord ventral horn motor neurons of both FALS patients and mutant *SOD1* transgenic mice. Two-hybrid screening for the physiological targets of NEDL1 has identified Dishevelled-1, one of the key transducers in the Wnt signaling pathway. Mutant SOD1 also interacted with Dishevelled-1 in the presence of NEDL1 and caused its dysfunction. Thus, our results suggest that an adverse interaction among misfolded SOD1, NEDL1, translocon-associated protein-δ, and Dishevelled-1 forms a ubiquitinated protein complex that is included in potentially cytotoxic protein aggregates and that mutually affects their functions, leading to motor neuron death in FALS.

Amyotrophic lateral sclerosis (ALS)[1] is a progressive, fatal, neurodegenerative disease that is characterized by selective loss of motor neurons in the spinal cord, brain stem, and motor cortex. The sporadic and familial forms of the disease have similar clinical and pathological features. About 10% of ALS cases are familial, and mutation of superoxide dismutase-1 (SOD1) is found in 20% of familial ALS (FALS) patients (1, 2). Mice that express mutant *SOD1* transgenes develop an age-dependent ALS phenotype independent of levels of dismutase activity, suggesting that FALS pathology is because of a toxic gain of function in SOD1 and that the abnormal protein structure of mutant SOD1 is critical in the pathogenesis of motor neuron death (3–6). Recently, proteasome expression and activity have been reported to decrease with age in the spinal cord (7, 8). Furthermore, mutant SOD1 turns over more rapidly than wild-type SOD1, and an inhibitor of proteasome action inhibits this turnover and thus selectively increases the steady-state level of mutant SOD1 (8). These results suggest the involvement of the ubiquitin-proteasome function in the cause of FALS. However, the biochemical nature of this gain-of-function mutation in SOD1 and the mechanism by which SOD1 mutations cause the degeneration of motor neurons have remained elusive.

We show here the identification of a novel HECT-type ubiquitin-protein isopeptide ligase (E3), NEDL1, which is expressed in neuronal tissues, including the spinal cord, and selectively binds to and ubiquitinates mutant (but not wild-type) SOD1. NEDL1 is physically associated with translocon-associated protein-δ (TRAP-δ), one of the endoplasmic reticulum (ER) translocon components that has previously been reported to bind mutant SOD1 (9, 10). Both NEDL1 and TRAP-δ form a complex with mutant SOD1, with the binding intensity among these proteins being roughly proportionate to the rapidity of progression of the associated FALS phenotype. Immunohistochemical study has shown that NEDL1 is positive in the Lewy body-like hyaline inclusions in the spinal cord motor neurons of both FALS patients and mutant *SOD1* transgenic mice. We have also found that NEDL1 targets Dishevelled-1 (Dvl1) for ubiquitination-mediated degradation and that mutant (but not wild-type) SOD1 affects the function of Dvl1. Our observations suggest that NEDL1 is a quality control E3 that recognizes mutant SOD1 to form a tight complex with the physiological targets of NEDL1 in motor neurons of FALS patients.

EXPERIMENTAL PROCEDURES

Cell Culture and Transfection—Human neuroblastoma-derived cells were grown in RPMI 1640 medium supplemented with 10% heat-inactivated fetal bovine serum, 100 units/ml penicillin, and 100 μg/ml streptomycin. COS-7 and Neuro2a cells were maintained in Dulbecco's modified Eagle's medium supplemented with 10% heat-inactivated fe-

* This work was supported in part by Hisamitsu Pharmaceutical Co. Inc. (to A. N.), by grants from the Ministry of Health, Labor, and Welfare of Japan (to A. N. and Y. I.), and by grants from the Ministry of Education, Culture, Sports, Science, and Technology of Japan (to A. N., Y. I., and M. A.). The costs of publication of this article were defrayed in part by the payment of page charges. This article must therefore be hereby marked "*advertisement*" in accordance with 18 U.S.C. Section 1734 solely to indicate this fact.

The nucleotide sequence(s) reported in this paper has been submitted to the GenBank™/EBI Data Bank with accession number(s) AB048365 (Nbla0078 and human NEDL1), AB002320 (KIAA0322), and AB083710 (mouse Nedl1).

** To whom correspondence should be addressed: Div. of Biochemistry, Chiba Cancer Center Research Inst., 666-2 Nitona, Chuoh-ku, Chiba 260-8717, Japan. Tel.: 81-43-264-5431; Fax: 81-43-265-4459; E-mail: akiranak@chiba-ccri.chuo.chiba.jp.

[1] The abbreviations used are: ALS, amyotrophic lateral sclerosis; FALS, familial amyotrophic lateral sclerosis; SOD1, superoxide dismutase-1; E3, ubiquitin-protein isopeptide ligase; NEDL1, NEDD4-like ubiquitin-protein ligase-1; TRAP-δ, translocon-associated protein-δ; ER, endoplasmic reticulum; Dvl1, Dishevelled-1; RT, reverse transcription; LBHI, Lewy body-like hyaline inclusion; JNK, c-Jun N-terminal kinase; HECT domain, homologous to E6AP carboxyl-terminus.

tal bovine serum, 100 units/ml penicillin, and 100 μg/ml streptomycin. All cells were maintained in a humidified 37 °C incubator with 5% CO_2. All transfections were carried out with LipofectAMINE Plus transfection reagent (Invitrogen) according to the manufacturer's instructions. In some experiments, transfected cells were treated with MG-132 for 30 min at a final concentration of 40 μM.

RNA Analysis—A human multiple tissue mRNA blot and a fetal human multiple mRNA blot (Invitrogen) were hybridized with a ^{32}P-labeled ApaI-ScaI restriction fragment of *NEDL1* cDNA under standard conditions. For reverse transcription (RT)-PCR analysis, cDNA derived from adult human neural system (BioChain Institute, Hayward, CA) was subjected to PCR amplification using the following primers: *NEDL1*, 5′-CCGATTTGAGATCACTTCCTCC-3′ (sense) and 5′-CCGCTTTCCATCAGGTTGTT-3′ (antisense); and glyceraldehyde-3-phosphate dehydrogenase, 5′-ACCTGACCTGCCGTCTAGAA-3′ (sense) and 5′-TCCACCACCCTGTTGCTGTA-3′ (antisense). The amplified products were separated by electrophoresis on a 1.5% agarose gel and visualized by ethidium bromide post-staining. Amplification of glyceraldehyde-3-phosphate dehydrogenase was used as an internal control.

In Vitro Ubiquitination Assays—*In vitro* ubiquitination assays were performed as follows. Reaction mixtures containing 0.5 μg of purified glutathione *S*-transferase fusion proteins, 0.25 μg of yeast ubiquitin-activating enzyme (*E1*) (BostonBiochem, Cambridge, MA), 1 μl of crude lysates from *Escherichia coli* expressing ubiquitin carrier proteins (*E2*), and 10 μg of bovine ubiquitin (Sigma) were incubated in 250 mM Tris-HCl (pH 7.6), 1.2 M NaCl, 50 mM ATP, 10 mM $MgCl_2$, and 30 mM dithiothreitol. Reactions were terminated after 2 h at 30 °C by the addition of SDS sample buffer. Samples were resolved by SDS-PAGE, transferred to membranes, and immunoblotted with anti-ubiquitin monoclonal antibody 1B3 (Medical & Biological Laboratories, Nagoya, Japan).

Immunofluorescence Staining—Cells grown on coverslips were processed for immunofluorescence. Briefly, cells were fixed in 3.7% formaldehyde, permeabilized in 0.2% Triton X-100, and finally incubated with anti-NEDL1 antibody (diluted 1:100). The primary antibody was detected with fluorescein isothiocyanate-conjugated goat anti-rabbit IgG (diluted 1:500; Jackson ImmunoResearch Laboratories, Inc., West Grove, PA). Images were taken using an Olympus confocal microscopy system.

Yeast Two-hybrid Screening—Yeast two-hybrid screening was performed using the Gal4-based Matchmaker two-hybrid system with the cDNA libraries derived from fetal human brain (first screening) and adult human brain (second screening) (Clontech, Palo Alto, CA). *Saccharomyces cerevisiae* CG1945 cells were transformed with pAS2–1-NEDL1-1 (amino acids 757–1114; first screening) or pAS2–1-NEDL1-2 (amino acids 382–1448; second screening), which did not activate the transcription of *lacZ* alone. The transformants were subsequently transformed with the cDNA library, and the *lacZ*-positive colonies were selected. The plasmid DNAs were extracted from these positive colonies, and their nucleotide sequences were determined.

Immunoprecipitation and Western Blot Analysis—Anti-NEDL1 and anti-TRAP-δ polyclonal antibodies were raised in rabbits against an NEDL1 oligopeptide (amino acids 460–482) and a TRAP-δ oligopeptide (amino acids 93–126), respectively. For immunoprecipitation, COS-7 or Neuro2a cells were cotransfected with the expression plasmids in various combinations and lysed 48 h later in 10 mM Tris-HCl (pH 7.8), 150 mM NaCl, 1% Nonidet P-40, 1 mM EDTA, and 1 mM phenylmethylsulfonyl fluoride supplemented with protease inhibitor mixture (Sigma). Whole cell lysates were immunoprecipitated with anti-NEDL1, anti-FLAG (M2; Sigma), or anti-Myc (9B11; Cell Signaling Technology, Beverly, MA) antibody. Immune complexes were recovered on protein G-Sepharose beads, eluted by boiling in Laemmli sample buffer, electrophoresed on SDS-polyacrylamide gel, and then transferred to a polyvinylidene difluoride membrane (Immobilon, Millipore Corp., Bedford, MA) by electroblotting. For ubiquitination experiments, cell lysis was performed in radioimmune precipitation assay buffer (10 mM Tris-HCl (pH 7.4), 150 mM NaCl, 1% Nonidet P-40, 0.1% sodium deoxycholate, 0.1% SDS, and 1 mM EDTA), followed by strong sonication and freeze-thaw. The membrane was probed with the indicated primary antibodies and then incubated with the appropriate secondary antibodies labeled with horseradish peroxidase (Jackson ImmunoResearch Laboratories, Inc. and Southern Biotechnology Associates, Inc., Birmingham, AL). Immunoreactive bands were detected by the enhanced chemiluminescence technique (ECL, Amersham Biosciences). For the detection of c-Jun phosphorylation, we used anti-c-Jun (sc-45, Santa Cruz Biotechnology, Santa Cruz, CA) or anti-phospho-Ser^{63} c-Jun (Cell Signaling Technology) antibody.

Cloning of Human NEDL1 cDNA—A forward primer (5′-GGTTTTTAGGCCTGGCCGCC-3′) and a reverse primer (5′-CAATGAGGTACATGCCAATCC-3′) were used to amplify the 5′-part of the *NEDL1* cDNA using cDNA libraries derived from human neuroblastoma and fetal human brain (Stratagene, La Jolla, CA) as templates. The full-length human *NEDL1* cDNA was generated by fusion of the PCR-amplified fragment (nucleotides +1 to +68, where position +1 represents the translation initiation site) and the *KIAA0322* cDNA (a gift from T. Nagase, Kazusa DNA Institute). Gel electrophoresis and Western blot analysis were carried out as described above.

Expression Constructs—The mammalian expression plasmids for hemagglutinin-tagged and His_6-tagged ubiquitin were kind gifts of D. Bohmann. The full-length *NEDL1* cDNA was inserted into the mammalian expression plasmid pEF1/His (Invitrogen) or pIRESpuro2 (Clontech). cDNAs encoding wild-type and mutant forms of SOD1 were fused to the FLAG or Myc epitope tag sequence at their C termini and subcloned into pIRESpuro2. Similarly, the FLAG or Myc epitope tag sequence was attached to the C terminus of TRAP-δ. Also similarly, the FLAG or Myc epitope tag sequence was attached to the N terminus of Dvl1. Coding sequences were verified by automated DNA sequencing.

Protein Stability Experiments—Neuro2a cells were transfected with the expression plasmid for the wild-type or mutant form of SOD1 with or without the NEDL1 expression plasmid. Twenty-four hours after transfection, cycloheximide (50 μg/ml) was added to the culture medium, and the cells were harvested at the indicated time points by lysis in radioimmune precipitation assay buffer. The protein concentrations were determined using the Bradford protein assay system (Bio-Rad) according to the instructions of the manufacturer.

Immunohistochemistry—The immunohistochemical studies were performed as described previously using affinity-purified rabbit anti-NEDL1 antibody (11). Patient tissues were obtained at autopsy from two FALS siblings from a Japanese family. The clinical course of the sister, who died at age 46, was 18 months (case 1), and that of the brother, who died at age 65, was 11 years (case 2) (11). The *SOD1* gene was mutated with a 2-bp deletion at codon 126 (11, 12). Normal spinal cord tissues were obtained from three neurologically and neuropathologically normal individuals. The same study was performed on spinal cord tissues from three normal rats and a transgenic ALS rat carrying a mutant allele of the human *SOD1* gene (H46R) (13). These mice were killed at 180 days. As a negative control, some sections were incubated with anti-NEDL1 antibody that had been pre-absorbed with an excess of NEDL1 antigen. Bound antibodies were visualized by the avidin-biotin-immunoperoxidase complex method.

RESULTS

Cloning and Expression of the NEDL1 E3 Gene—To detect novel molecules that are important in regulating neuronal programmed cell death, we constructed oligo-capping cDNA libraries from a mixture of three fresh human neuroblastoma tissues (stages 1 and 2) that were undergoing gradual spontaneous regression, probably by neuronal apoptosis (14). Screening of 1152 novel genes by RT-PCR revealed that 194 genes were expressed differentially in regressing neuroblastomas with favorable prognosis and in aggressive tumors with poor prognosis. Among these genes, we found a partial cDNA sequence with an HECT-like domain (*Nbla0078*) that partially matched the *KIAA0322* gene. Because *KIAA0322* lacks a 5′-coding region, we used a genome-based PCR procedure to clone the corresponding full-length cDNA. This is predicted to encode a protein product of 1585 amino acids with homology to NEDD4 E3 (15, 16), which includes a C2 domain at the N-terminal region supposed to mediate its membrane localization in a calcium-dependent manner, two WW motifs important for protein-protein interaction through binding to specific proline-rich clusters, and a conserved catalytic HECT domain at the C terminus (Fig. 1*A*). We named this novel ligase, which mapped to chromosome 7p13, NEDL1 (NEDD4-like ubiquitin-protein ligase-1). We also cloned the mouse counterpart of *NEDL1* cDNA, whose amino acid sequence is 78% identical to the human sequence. Tissue-specific expression of *NEDL1* mRNA of ~10 and 7 kb in size was observed, with predominant expression in adult and fetal brains as examined by Northern blot analysis (Fig. 1*B*). Its

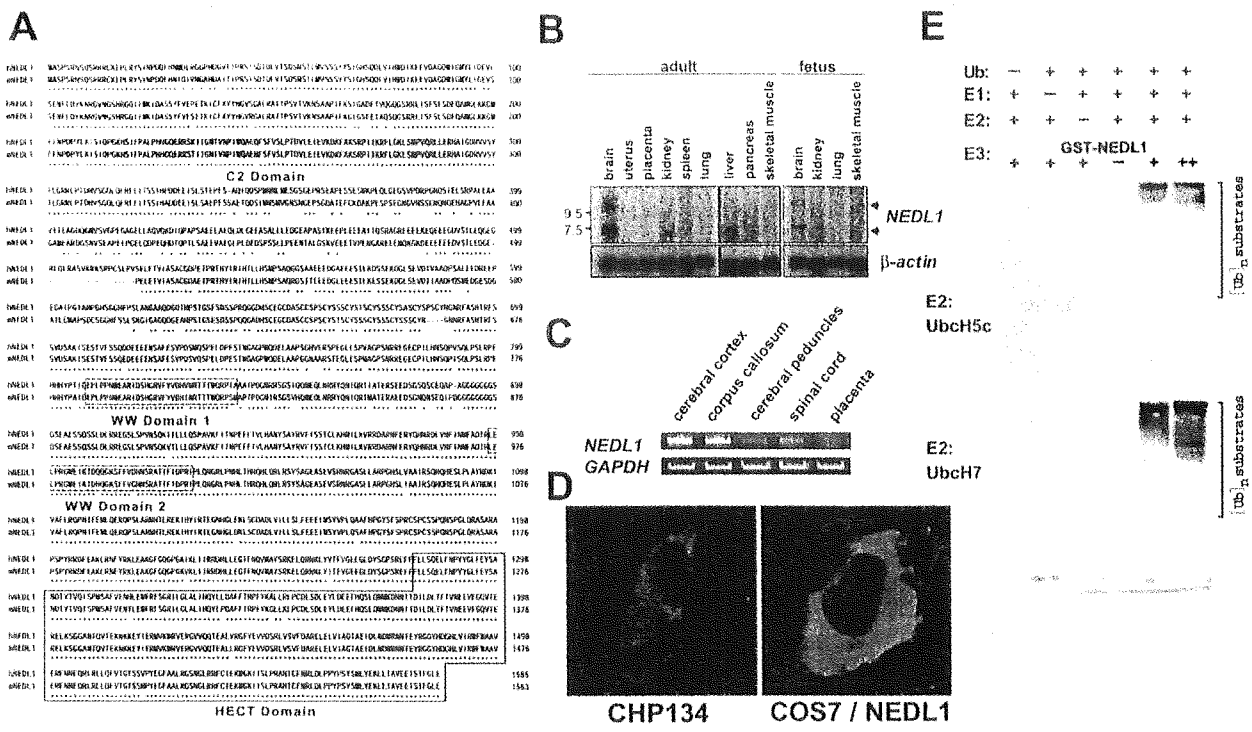

FIG. 1. **Amino acid sequence, brain-specific expression, and subcellular localization of NEDL1 E3.** *A*, alignment of conserved amino acid sequences of human NEDL1 (*hNEDL1*) and its mouse homolog (*mNEDL1*). *Numbers* on the right indicate the number of residues to the initiator methionine. The C2 domain (*shaded*), two WW domains (*dashed boxes*), and the HECT domain (*solid box*) are indicated. *B*, brain-specific expression of *NEDL1* mRNA. Total RNAs derived from the indicated adult (*left panel*) and fetal (*right panel*) human tissues were analyzed by Northern blotting using a ^{32}P-labeled human *NEDL1* cDNA restriction fragment as a probe. Control hybridization with a human β-actin cDNA probe verified the equal amount of RNA loaded. *C*, expression of *NEDL1* in human brain subsections. Total RNA from the cerebral cortex, corpus callosum, cerebral peduncles, spinal cord, or placenta was subjected to RT-PCR using specific primers for *NEDL1* or glyceraldehyde-3-phosphate dehydrogenase (*GAPDH*). RT-PCR analysis for *NEDL1* in the placenta provided a negative control. Amplification of glyceraldehyde-3-phosphate dehydrogenase was used as an internal control. *D*, confocal microscopic images of human neuroblastoma CHP134 cells (*left panel*) and COS-7 cells transfected with an expression plasmid for NEDL1 (*right panel*). Cells were subjected to immunofluorescence analysis using rabbit anti-NEDL1 polyclonal antibody, followed by fluorescein isothiocyanate-conjugated anti-mouse IgG. E, *in vitro* ubiquitination assays showing that NEDL1 has a ubiquitin-protein ligase activity. The degree of ubiquitination was increased in an NEDL1-dependent manner. In this assay, yeast ubiquitin-activating enzyme (*E1*), bacterially expressed ubiquitin carrier protein (*E2*; UbcH5C or UbcH7), and bacterial lysates were incubated in the presence or absence of increasing amounts of glutathione *S*-transferase (*GST*)-NEDL1. Polyubiquitinated bacterial proteins appeared to migrate in a high molecular mass complex. *Ub*, ubiquitin.

expression was also weakly detected in adult kidney, where the size of the expressed transcript appeared to be <7 kb. Expression of *NEDL1* in specific regions of the nervous system was further confirmed in the cerebral cortex, corpus callosum, cerebral peduncles, and spinal cord by RT-PCR (Fig. 1*C*). Thus, NEDL1 is a novel HECT-type E3 preferentially expressed in neuronal tissues, including the spinal cord. Using a specific anti-NEDL1 polyclonal antibody that we generated, we localized NEDL1 primarily to the cytoplasm in both intact human neuroblastoma CHP134 cells and COS-7 cells transiently expressing NEDL1 (Fig. 1*D*). The *in vitro* system containing UbcH5c or UbcH7 demonstrated that NEDL1 has a ubiquitin-protein ligase activity (Fig. 1*E*).

NEDL1 Physically Interacts with TRAP-δ and Mutant SOD1—We then sought protein-binding partners of NEDL1 by yeast two-hybrid screening using the region including two WW protein interaction domains (amino acids 757–1114) as bait. Of 96 positive clones subjected to DNA sequencing, one was a full-length cDNA for TRAP-δ; this was of considerable interest, as TRAP-δ was previously reported to bind mutant (G85R and G93A), but not wild-type, SOD1 (9). TRAP-δ is a protein component of the translocon in the ER membrane (10). We therefore examined the interaction among NEDL1, TRAP-δ, and SOD1 by an immunoprecipitation assay after cotransfecting the corresponding expression constructs into COS-7 cells. As shown in Fig. 2 (*A* and *B*), NEDL1 was physically associated with both exogenous and endogenous TRAP-δ probably through the region of two WW domains, as originally suggested by the result of two-hybrid screening. Surprisingly, NEDL1 bound to mutant (but not wild-type) SOD1 (Fig. 2*C*). Furthermore, the degree of binding between NEDL1 and different mutant SOD1 proteins was roughly proportionate to the rapidity of progression (time from clinical onset to death) of the associated FALS phenotype (17–23). For example, two mutant SOD1 proteins associated with an extremely rapid clinical course (C6F and A4V) interacted very strongly with NEDL1. By contrast, the binding of NEDL1 to other mutants was less striking and decreased proportionately to the falloff of disease severity corresponding to those mutants. Of further interest, like the NEDL1-mutant SOD1 interaction, the binding intensity between TRAP-δ and mutant SOD1 was also dependent on the disease severity (Fig. 2*D*). These observations suggest that NEDL1 and TRAP-δ are normally associated with each other, but that misfolded mutant SOD1 makes a complex with them. Such a complex is not formed with wild-type SOD1. The experiments using the *in vitro* translated proteins suggested that association of mutant SOD1 and TRAP-δ was direct (data not shown). It therefore appears that mutant SOD1 forms tightly bound protein complexes with NEDL1 and TRAP-δ and that the tightness of binding in the complex is determined in part by

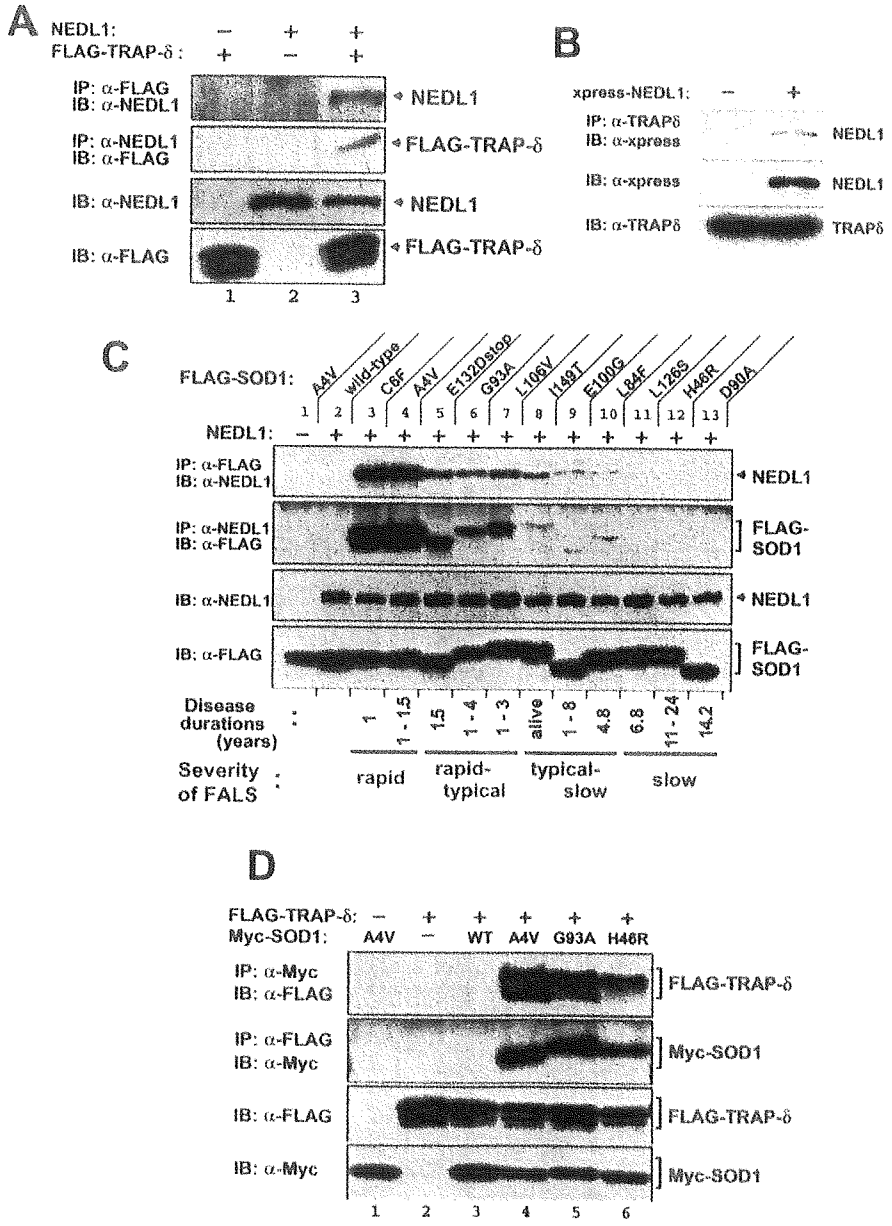

FIG. 2. **NEDL1 interacts with TRAP-δ and FALS-associated mutant forms of SOD1, but not with wild-type SOD1.** *A*, NEDL1 interacts with TRAP-δ. COS-7 cells were cotransfected with the indicated expression plasmids, and whole cell lysates were immunoprecipitated (*IP*) with anti-FLAG (*first panel*) or anti-NEDL1 (*second panel*) antibody. Immunoprecipitates were analyzed by immunoblotting (*IB*) using the indicated antibodies. Whole cell lysates were analyzed for expression levels of each protein by immunoblot analysis (*third* and *fourth panels*). Detection was performed with horseradish peroxidase-conjugated secondary antibodies. *B*, NEDL1 also binds to endogenous TRAP-δ. *C*, interaction between NEDL1 and mutant SOD1. Whole cell lysates from COS-7 cells overexpressing NEDL1 and one of the FLAG-tagged SOD1 mutants or wild-type SOD1 were immunoprecipitated with anti-FLAG (*first panel*) or anti-NEDL1 (*second panel*) antibody and then immunoblotted with anti-NEDL1 or anti-FLAG antibody, respectively. The expression of NEDL1 or FLAG-tagged SOD1 mutants was analyzed by immunoblotting using anti-NEDL1 (*third panel*) or anti-FLAG (*fourth panel*) antibody, respectively. Patients carrying the SOD1(C6F) and SOD1(A4V) mutations have a rapid clinical course, whereas mutant SOD1(L126S), SOD1(H46R), or SOD1(D90A) is associated with a slow clinical course. *D*, interaction of TRAP-δ with mutant SOD1. COS-7 cells were transiently cotransfected with the expression plasmid for FLAG-tagged TRAP-δ and the expression plasmid encoding one of the Myc-tagged SOD1 mutants or wild-type (*WT*) SOD1. Whole cell lysates were immunoprecipitated with anti-Myc (*first panel*) or anti-FLAG (*second panel*) antibody, followed by immunoblotting with anti-FLAG or anti-Myc antibody, respectively. The levels of overexpression of FLAG-tagged TRAP-δ (*third panel*) and Myc-tagged SOD1 (*fourth panel*) were analyzed by immunoblotting using anti-FLAG and anti-Myc antibodies, respectively.

properties of the mutant enzyme that also modulate disease severity of the resulting ALS phenotype. Such complexes do not form in cells with wild-type SOD1.

Determination of the Interaction Domains—We next examined the domains of NEDL1 required for formation of the SOD1·NEDL1·TRAP-δ complex. We generated various constructs of NEDL1 with deletions of each domain. Fig. 3 shows the results of immunoprecipitation assay for the association between deletion mutants of NEDL1 and mutant SOD1(G93A). Mutant SOD1 bound weakly to NEDL1 lacking WW domain-1 (Fig. 3A), suggesting that WW domain-1 and its surrounding portion are the region involved in their interaction. Immuno-

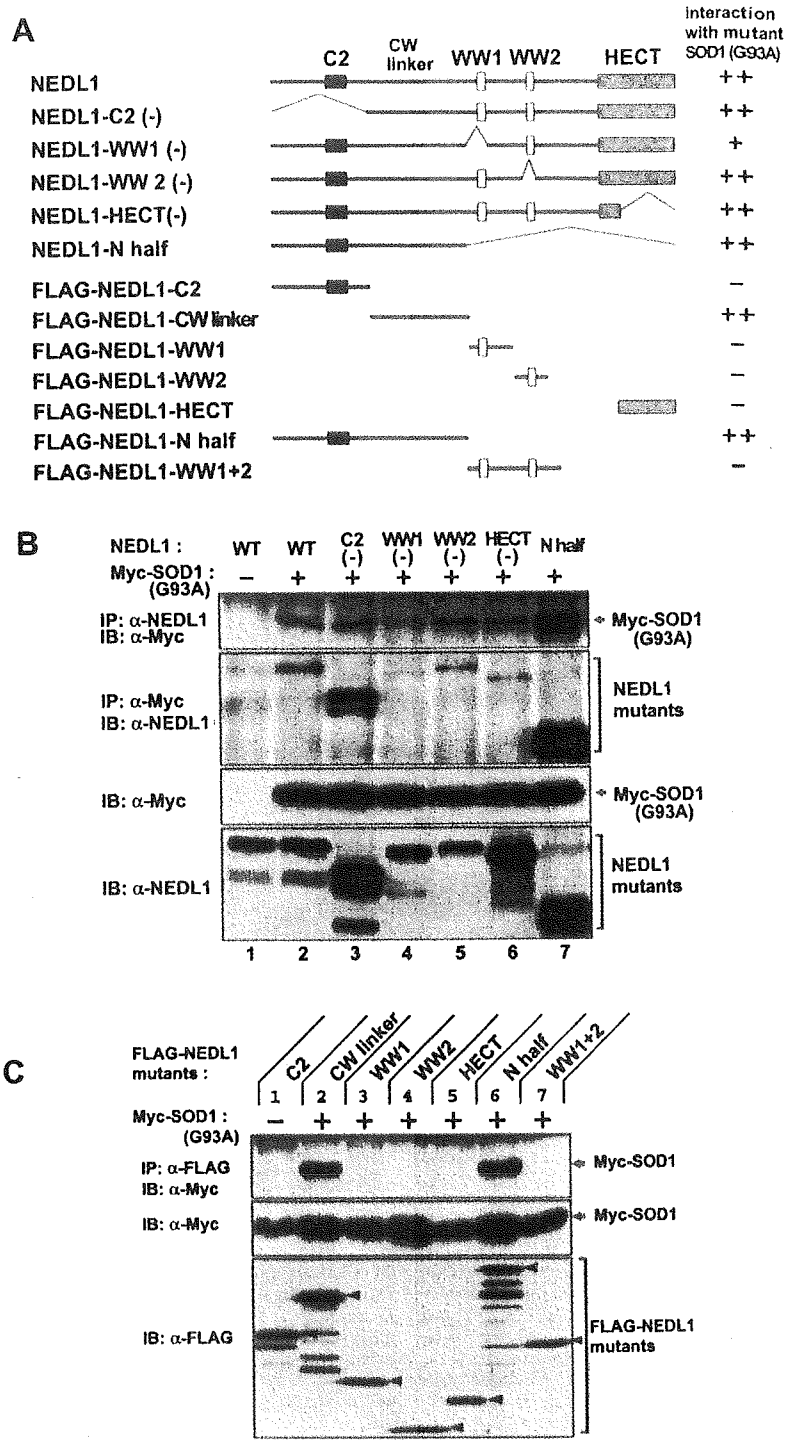

FIG. 3. **The region of NEDL1 between the C2 domain and WW domain-1 is required for interaction with mutant SOD1.** *A*, schematic illustration of wild-type NEDL1 and a series of deletion mutants of NEDL1. *CW linker* indicates the region between the C2 domain and WW domain-1 (*WW1*). *B* and *C*, immunoprecipitation and immunoblot analyses. In *B*, Myc-tagged mutant SOD1(G93A) was overexpressed together with wild-type (*WT*) NEDL1 or the indicated deletion mutants of NEDL1 in COS-7 cells. Whole cell lysates were immunoprecipitated (*IP*) with anti-NEDL1 (*first panel*) or anti-Myc (*second panel*) antibody, followed by immunoblotting (*IB*) with anti-Myc or anti-NEDL1 antibody, respectively. The expression levels of each protein were analyzed by immunoblotting using the indicated antibodies (*third* and *fourth panels*). In *C*, whole cell lysates were immunoprecipitated with anti-FLAG antibody and then immunoblotted with anti-Myc antibody (*upper panel*). Whole lysates were also analyzed by Western blotting for each protein (*middle* and *lower panels*).

precipitation analysis using the specific regions of NEDL1 clearly showed that the region between the C2 domain and WW domain-1 (CW linker region) is necessary for binding to mutant SOD1(G93A). Mutant SOD1(A4V) was also associated with NEDL1 through the same region, and TRAP-δ bound to the two WW domains of NEDL1 (data not shown).

NEDL1 Ubiquitinates Mutant SOD1 for Degradation Depending on the Disease Severity of FALS—Because NEDL1 is an E3, we next tested whether it ubiquitinates TRAP-δ and mutant SOD1 for degradation. As shown in Fig. 4*A*, NEDL1 clearly ubiquitinated mutant SOD1(A4V), but not TRAP-δ (data not shown). Furthermore, the degree of ubiquitination of mutant SOD1 by NEDL1 was dependent on the disease severity of FALS (A4V > G93A > H46R) (Fig. 4*A*). Fig. 4*B* shows the time course of degradation of wild-type and mutant SOD1 in the presence or absence of NEDL1. As reported previously (46), mutant SOD1 was degraded more rapidly than wild-type SOD1. NEDL1 did not affect wild-type SOD1 degradation. As expected from the co-immunoprecipitation and ubiquitination analyses, degradation of mutant SOD1 was stimulated by NEDL1 proportionately to the disease severity of FALS caused by the particular SOD1 mutant (A4V > G93A > H46R ≥

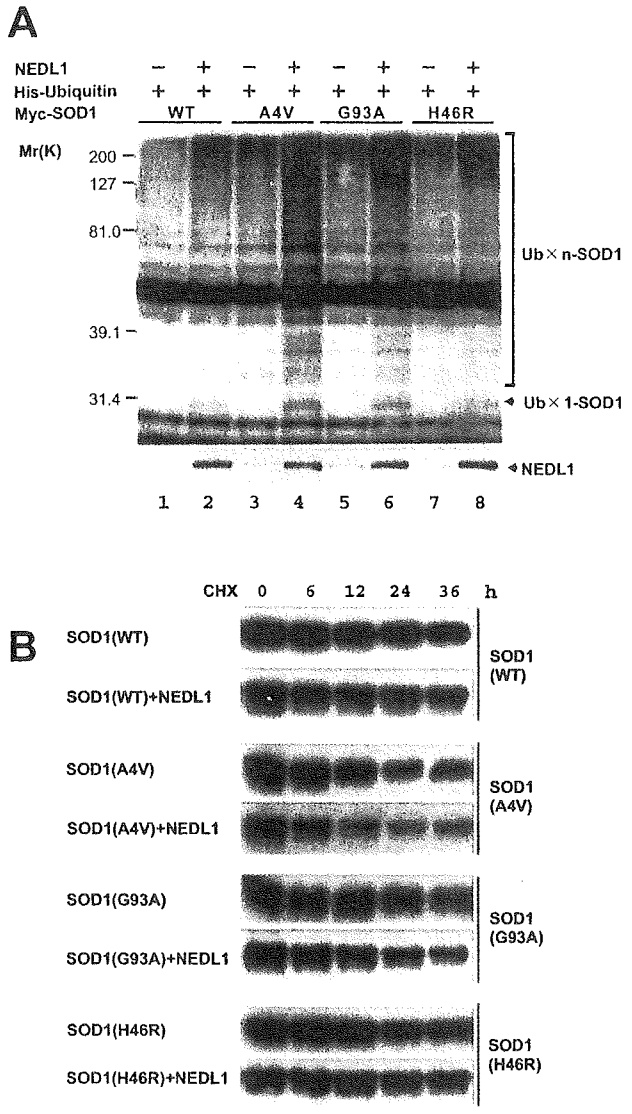

FIG. 4. **NEDL1-dependent ubiquitination and degradation of mutant forms of SOD1 correlate broadly with their respective clinical phenotypes.** *A*, NEDL1 ubiquitinates mutant SOD1 in a mutant type-dependent manner. COS-7 cells were transiently cotransfected with the indicated expression plasmids. Whole cell lysates from transfected COS-7 cells were immunoprecipitated with anti-Myc antibody, and immunoprecipitates were analyzed by Western blotting with anti-ubiquitin (*Ub*) antibody (*upper panel*). The *bracket* indicates slowly migrating ubiquitinated forms of SOD1. Whole cell lysates were analyzed by immunoblotting with anti-NEDL1 antibody to confirm the expression of transfected NEDL1 (*lower panel*). The running positions of molecular weight markers are indicated on the left. *B*, half-lives of wild-type (*WT*) and mutant SOD1 proteins in the presence or absence of NEDL1. Cell lysates were harvested from Neuro2a cells transfected with *SOD1* alone or with *SOD1* plus *NEDL1* at different time points as indicated after the addition of cycloheximide (*CHX*; final concentration of 50 μg/ml) and were analyzed for SOD1 protein levels by Western blotting with anti-FLAG antibody. In the presence of NEDL1, the half-lives of various mutant SOD1 proteins were reduced also roughly dependent on the disease severity of FALS (A4V > G93A > H46R).

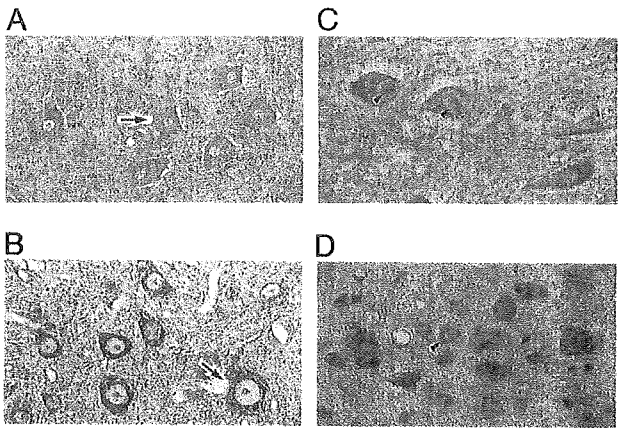

FIG. 5. **NEDL1 immunohistochemical analyses.** *A*, immunohistochemical analysis of NEDL1 in normal human spinal cord. NEDL1-positive anterior horn cells are evident (*arrow*), although the immunoreactivity for NEDL1 is somewhat faint. There was no counterstaining. Magnification ×520. *B*, NEDL1 immunohistochemistry in normal mouse spinal cord. Normal anterior horn cells are positive for NEDL1 (*arrow*). The section was counterstained with hematoxylin. Magnification ×750. *C*, immunostaining for NEDL1 in spinal cord LBHIs from an FALS patient with a frameshift 126 mutation in the *SOD1* gene. The NEDL1-positive reaction products were mostly restricted to the cores of the core and halo-type LBHIs (*arrowheads*). In the LBHI-bearing neurons and residual neurons, the antibody to NEDL1 also stained the neuronal cell body. There was no counterstaining. Magnification ×540. *D*, NEDL1 immunostaining in a spinal cord LBHI from an *SOD1*(H46R) transgenic mouse. An ill defined LBHI in the *SOD1*(H46R) transgenic mouse was positive for NEDL1; this ill defined LBHI shows a diffuse staining pattern (*arrowhead*). The staining intensity in the residual neurons stained by anti-NEDL1 antibody varied from neuron to neuron. The section was counterstained with hematoxylin. Magnification ×770.

wild-type). Thus, NEDL1 targeted mutant SOD1 for ubiquitin-mediated degradation in the cell in parallel with the binding intensity.

Immunohistochemistry—One of the characteristic cytopathological changes of mutant SOD1-linked FALS is the formation of neuronal Lewy body-like hyaline inclusions (LBHIs) that contain aggregates of SOD1 and ubiquitin (24). We therefore performed immunostaining to determine whether the NEDL1 protein is included within the LBHIs of the spinal cord motor neurons obtained from two siblings with FALS caused by frameshift 126 mutation of SOD1 (11, 12). One case had neuropathological findings compatible with FALS with posterior column involvement, whereas the other had multisystem degeneration in addition to motor neuron disturbance. We also performed NEDL1 immunostaining in specimens obtained from mutant *SOD1*(H46R) transgenic mice at 180 days, by which time they show clinical motor signs in the hind limbs (13). The specificity of the NEDL1 staining was confirmed by pretreating the specimens with an excess of NEDL1 antigen. NEDL1 immunoreactivity in the spinal cords of the human control cases was identical to that of normal mice: immunoreactivity was identified predominantly in the cytoplasm of the neurons of the spinal cords (Fig. 5, *A* and *B*). The LBHIs in the anterior horn cells of two FALS patients and transgenic mice showed equivalent immunoreactivity for NEDL1. Although the intensity of NEDL1 immunoreactivity in neuronal LBHIs varied, most of the LBHIs were immunoreactive for NEDL1 (Fig. 5, *C* and *D*). The reaction products were generally restricted to the cores of the core and halo-type LBHIs that showed eosinophilic cores with pale peripheral halos upon hematoxylin and eosin staining (Fig. 5*C*); by contrast, immunopositive NEDL1 in ill defined LBHIs was distributed throughout the inclusions (Fig. 5*D*). NEDL1 immunoreactivity in the residual neurons in humans and mice was identified primarily in cell bodies. Thus, NEDL1 immunostaining was clearly positive in the FALS-related LBHIs that were also positive for ubiquitin and SOD1 (data not shown).

NEDL1 Targets Dishevelled-1 for Ubiquitin-mediated Protein Degradation—We next hypothesized that the physiological function of NEDL1 to mediate ubiquitination is interfered with

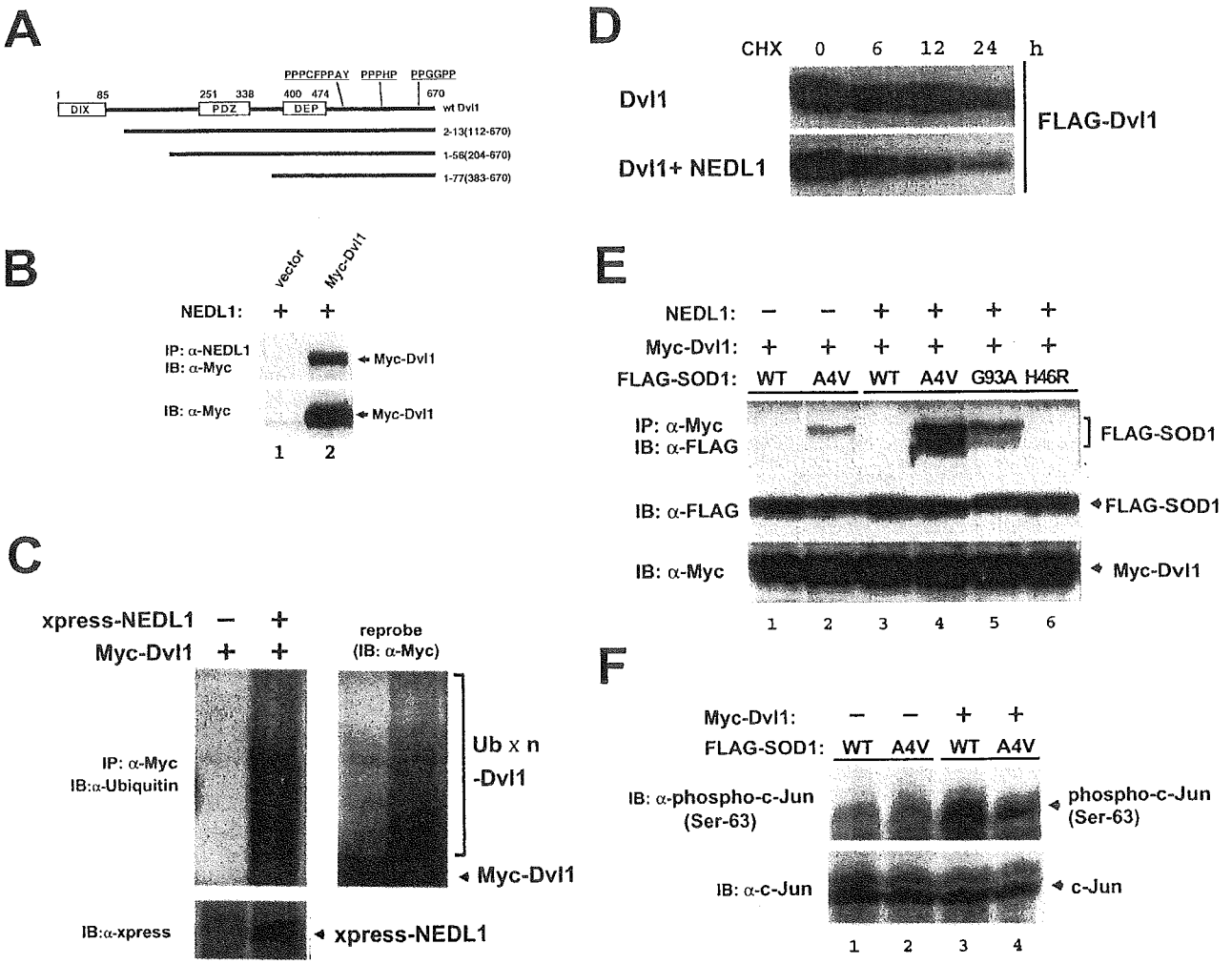

FIG. 6. **Dvl1 is a substrate of NEDL1, and its functions are disturbed by mutant SOD1(A4V).** *A*, schematic illustration of full-length Dvl1 and three clones obtained by yeast two-hybrid screening. Human Dvl1 consists of 670 amino acids and contains three conserved domains, including the DIX, PDZ, and DEP domains. Between the DEP domain and the C-terminal end, there are three proline-rich clusters, which might act as WW domain recognition sites. All three clones (clones 2–13, 1–56, 1–77) contain the DEP domain and these clusters. *B*, NEDL1 interacts with Dvl1. Myc-tagged Dvl1 was overexpressed together with NEDL1 in Neuro2a cells. Whole cell lysates were immunoprecipitated (*IP*) with anti-NEDL1 antibody, followed by immunoblotting (*IB*) with anti-Myc antibody (*upper panel*). The expression levels of Myc-tagged Dvl1 were analyzed by immunoblotting using anti-Myc antibody (*lower panel*). *C*, NEDL1 ubiquitinates Dvl1 in Neuro2a cells. The cells were transiently transfected with the indicated expression plasmids along with the ubiquitin expression plasmid in the presence or absence of the expression plasmid for XPRESS-tagged NEDL1. Whole cell lysates were immunoprecipitated with anti-Myc antibody and then immunoblotted with anti-ubiquitin antibody (*left panel*). The ladder of bands denoted by the *bracket* appeared to be ubiquitinated Dvl1. The expression of XPRESS-NEDL1 was analyzed by immunoblotting using anti-XPRESS antibody. The membrane was reprobed with anti-Myc antibody (*right panel*). *D*, Dvl1 is degraded by NEDL1. Neuro2a cells were transfected with the expression plasmid for FLAG-tagged Dvl1 with or without the NEDL1 expression plasmid. Transfected cells were harvested at different time points as indicated after the addition of cycloheximide (*CHX*; final concentration of 50 μg/ml), and Dvl1 protein levels were analyzed by Western blotting with anti-FLAG antibody. In the presence of NEDL1, the half-lives of FLAG-Dvl1 were significantly reduced. *E*, Dvl1 binds to mutant SOD1(A4V), and the degree of its binding is enhanced in the presence of NEDL1. Whole cell lysates prepared from COS-7 cells transfected with the indicated combinations of expression plasmids were subjected to immunoprecipitation and Western analyses as indicated. *F*, c-Jun phosphorylation by overexpression of Dvl1 is suppressed upon coexpression of mutant SOD1(A4V). Whole cell lysates from COS-7 cells transfected with the indicated combinations of expression plasmids were subjected to Western blotting with antibody against the phosphorylated form of c-Jun (*upper panel*) or with anti-c-Jun antibody (*lower panel*). *wt/WT*, wild-type.

by mutant SOD1. To test this hypothesis, we again performed yeast two-hybrid screening to obtain NEDL1-interacting molecules using the large region of NEDL1 (amino acids 382–1448) as bait. Of 396 His and β-galactosidase double-positive clones, 282 clones were subjected to DNA sequencing, and we identified Dvl1 (three clones). Human Dvl1 is a 670-amino acid protein with three conserved domains: a DIX domain, which is required for canonical Wnt/T-cell factor signaling; a PDZ domain, which is a target of both Stbm and casein kinase I binding; and a DEP domain, which is responsible for Dvl membrane localization during planar cell polarity signaling (25–27). Between the DEP domain and C-terminal end, there are three proline-rich clusters unique to mammalian Dvl1, which presumably act as the WW domain recognition sites. All three clones (clones 2–13, 1–56, and 1–77) contain the DEP domain and proline-rich clusters, suggesting that NEDL1 interacted with Dvl1 in the C-terminal half (Fig. 6*A*). In Neuro2a cells, NEDL1 co-immunoprecipitated with Dvl1 (Fig. 6*B*) and ubiquitinated it for degradation (Fig. 6, *C* and *D*). Thus, Dvl1 may be one of the physiological targets of NEDL1 E3. As recent studies strongly suggest that the cytotoxicity of SOD1 mutants is responsible for their aggregate properties, incorporating other proteins essential for cells into their aggregates (28), we examined the association between mutant SOD1 and Dvl1,

both of which interact with NEDL1. Of interest, Dvl1 bound to mutant SOD1(A4V), and complex formation was increased in the presence of NEDL1 roughly proportionately to the disease severity of FALS caused by the particular SOD1 mutant (Fig. 6*E*). Dvl1 is known to transduce not only the Wnt/β-catenin/T-cell factor pathway, but also the JNK/c-Jun pathway (27). Therefore, we next examined whether the Dvl1-induced phosphorylation of c-Jun at Ser^{63} was affected by the tight complex formation induced by inclusion of mutant SOD1. As shown in Fig. 6*F*, c-Jun phosphorylation induced by overexpression of Dvl1 was significantly suppressed by coexpression with mutant SOD1(A4V) in COS-7 cells.

DISCUSSION

Our present results demonstrate that a novel HECT-type NEDL1 E3, which is preferentially expressed in neuronal tissues, specifically targets mutant forms of SOD1 for ubiquitination-mediated protein degradation. NEDL1 is also associated with TRAP-δ localized at the ER translocon. The TRAP complex has recently been shown to facilitate the initiation of protein translocation in a substrate-specific manner (29). The NEDL1·TRAP-δ complex recognizes mutant (but not wild-type) SOD1, with a binding intensity that broadly parallels the disease severity of FALS. NEDL1 immunoreactivity was detected in the FALS-related LBHIs in the spinal cord ventral horn motor neurons, suggesting that, although mutant SOD1 is ubiquitinated for degradation by NEDL1, the mutant SOD1·NEDL1·TRAP-δ complex aggregates within the LBHIs. It is also conceivable that fragmentation of the Golgi apparatus reported in ALS patients and transgenic mice might be related to this aggregation (30, 31). These findings suggest possible hypotheses for the role of NEDL1 in the pathogenesis of FALS: 1) NEDL1, alone or with TRAP-δ, ubiquitinates and aggregates mutant SOD1, thereby decreasing the function of mutant SOD1; 2) NEDL1 and TRAP-δ form aggregates with mutant SOD1 that induce fragmentation of the Golgi apparatus, leading to neuronal apoptosis; 3) formation of these aggregates causes dysfunction of NEDL1 and/or TRAP-δ, and this, in turn, induces disturbances that ultimately cause motor neuron death; and 4) the mutant SOD1·NEDL1·TRAP-δ aggregates trap and inactivate unknown factor(s) such as molecular chaperones whose normal function is important for motor neuron viability.

To further understand the role of NEDL1 in motor neuron death, we searched for the physiological targets of NEDL1 and identified Dvl1. As expected, Dvl1 is ubiquitinated for degradation by NEDL1. Surprisingly, however, Dvl1 also interacts with mutant SOD1 in the presence of NEDL1 roughly proportionately to the disease severity of FALS caused by the particular SOD1 mutant. Dvl1, an essential multimodule signal transducer localized in the cellular cytosol and cytoskeleton, mediates planar cell polarity signaling as well as canonical Wnt/β-catenin signaling (27, 32). In mammals, three Dvl family members have so far been reported, and the level of Dvl1 expression is high in neuronal tissues (33). As far as we know, NEDL1 is the first E3 for Dvl1, interacting with the C-terminal region containing three proline-rich clusters. A recent report suggests that Dvl1 regulates microtubule stability through inhibition of glycogen synthase kinase-3β (34). Because cytoskeletal abnormalities have been reported in ALS motor neurons (35), it is possible that the effect of mutant SOD1 on NEDL1-mediated Dvl1 degradation is involved in the motor neuron death. Furthermore, Dvl1 is abundant in the postsynaptic membrane region at the neuromuscular junction (36) that is reported to be involved in several neurodegenerative disorders (37, 38). Of interest, *Dvl1* is mapped to chromosome 1p36, which is a commonly deleted region in many human cancers, including neuroblastoma (39). As NEDL1 is highly expressed in neuroblastomas with favorable prognosis, which have a tendency to differentiate and/or regress, NEDL1 may be involved in the regulation of neuronal differentiation and survival possibly by controlling Dvl1.

NEDL1, TRAP-δ, mutant SOD1, and Dvl1 appear to form a complex roughly proportionately to the disease severity of FALS caused by the particular SOD1 mutant. Our present observations strongly suggest that NEDL1 may be a quality control E3 recognizing misfolded mutant SOD1 (40). The association between mutant SOD1 and NEDL1 may induce the conformational change in the NEDL1 protein to increase the binding intensity with other physiological targets such as TRAP-δ (not ubiquitinated) and Dvl1 (ubiquitinated). This may lead to tight complex formation especially when the proteasome activity is impaired. It has been reported that the expression and function of proteasomes decrease with age in the spinal cord (7). Okado-Matsumoto and Fridovich (41) have also found that complex formation between mutant SOD1 and heat shock proteins leads to protein aggregates. Because our data show that the ER translocon component TRAP-δ is involved, aggregate formation may occur at the sites of the ER or Golgi apparatus or even at other cellular sites. The complex formation including NEDL1 and mutant SOD1 may conversely affect the physiological function of NEDL1, as demonstrated by a decrease in Dvl1-induced phosphorylation of c-Jun.

Recently, the RING finger-type E3 Dorfin has been reported to ubiquitinate mutant SOD1 for degradation (42). However, NEDL1 and Dorfin appear to be different in several aspects. First, NEDL1 is expressed specifically in neuronal tissues, including the spinal cord, whereas Dorfin is ubiquitously expressed in most human tissues. Second, both interaction between NEDL1 and mutant SOD1 and ubiquitination of the latter by NEDL1 roughly parallel the disease severity caused by the particular SOD1 mutant, whereas Dorfin similarly ubiquitinates mutant forms of SOD1. In addition, we have identified Dvl1 and TRAP-δ as cellular target proteins of NEDL1, whereas the physiological targets of Dorfin have never been reported. It is probable that there are some other E3 ligases targeting mutant SOD1. However, the molecular characteristics, including tissue-specific expression, subcellular localization, and age-dependent expression, might be important in the development of the FALS phenotype.

In conclusion, we have identified a novel neuronal E3 (NEDL1) that interacts with TRAP-δ and also binds to and ubiquitinates Dvl1 for degradation. Strikingly, NEDL1 targets and ubiquitinates mutant (but not wild-type) SOD1 for degradation. NEDL1 may normally function in the quality control of cellular proteins by eliminating misfolded proteins such as mutant SOD1, possibly via a mechanism analogous to that of ER-associated degradation (43–45). NEDL1 appears to complex tightly with mutant SOD1, Dvl1, and TRAP-δ, forming aggregates with species of mutant SOD1 that have escaped ubiquitin-mediated degradation. The NEDL1 function that affects the activities of the target proteins may also be modulated by mutant SOD1. All of these might contribute to the pathogenesis of FALS; further elucidation of the molecular mechanism of formation of this complex and its pathogenicity may provide insights into motor neuron death in ALS as well as possible new therapeutic strategies for ALS.

Acknowledgments—We thank Robert H. Brown, Jr. (Harvard Medical School) for critical comments and reading the manuscript. We also thank M. Ohira and Y. Nakamura for helping with cDNA cloning and sequencing; K. Watanabe and M. Suzuki for making plasmid constructs; M. Nagai and M. Kato for helping with immunohistochemical studies; S. Hatakeyama, M. Matsumoto, and K. Nakayama

for ubiquitination assay instruction; and S. Sakiyama for reading the manuscript.

REFERENCES

1. Rosen, D. R., Siddique, T., Patterson, D., Figlewicz, D. A., Sapp, P., Hentati, A., Donaldson, D., Goto, J., O'Regan, J. P., Deng, H. X., Rahmani, Z., Krizus, A., McKenna-Yasek, D., Cayabyab, A., Gaston, S. M., Berger, R., Tanzi, R. E., Halperin, J. J., Herzfeldt, B., van den Bergh, R., Hung, W.-Y., Bird, T., Deng, G., Mulder, D. W., Smyth, C., Laing, N. G., Soriano, E., Pericak-Vance, M. A., Haines, J., Rouleau, G. A., Gusella, J. S., Horvitz, H. R., and Brown, R. H., Jr. (1993) *Nature* **364,** 59–62
2. Deng, H. X., Hentati, A., Tainer, J. A., Iqbal, Z., Cayabyab, A., Hung, W.-Y., Getzoff, E. D., Hu, P., Herzfeldt, B., Roos, R. P., Warner, C., Deng, G., Soriano, E., Smyth, C., Parge, H. E., Ahmed, A., Roses, A. D., Hallewell, R., Rericak-Vance, M. A., and Siddique, T. (1993) *Science* **261,** 1047–1051
3. Cleveland, D. W., and Liu, J. (2001) *Nat. Med.* **6,** 1320–1321
4. Brown, R. H., Jr., and Robberecht, W. (2001) *Semin. Neurol.* **21,** 131–139
5. Cluskey, S., and Ramsden, D. B. (2001) *Mol. Pathol.* **54,** 386–392
6. Orrell, R. W., and Figlewicz, D. A. (2001) *Neurology* **57,** 9–17
7. Keller, J. N., Huang, F. F., and Markesbery, W. R. (2000) *Neuroscience* **98,** 149–156
8. Hoffman, E. K., Wilcox, H. M., Scott, R. W., and Siman, R. (1996) *J. Neurol. Sci.* **139,** 15–20
9. Kunst, C. B., Mezey, E., Brownstein, M. J., and Patterson, D. (1997) *Nat. Genet.* **15,** 91–94
10. Hartmann, E., Gorlich, D., Kostka, S., Otto, A., Kraft, R., Knespel, S., Burger, E., Rapoport, T. A., and Prehn, S. (1993) *Eur. J. Biochem.* **214,** 375–381
11. Kato, S., Shimoda, M., Watanabe, Y., Nakashima, K., Takahashi, K., and Ohama, E. (1996) *J. Neuropathol. Exp. Neurol.* **55,** 1089–1101
12. Kato, S., Hayashi, H., Nakashima, K., Nanba, E., Kato, M., Hirano, A., Nakano, I., Asayama, K., and Ohama, E. (1997) *Am. J. Pathol.* **151,** 611–620
13. Nagai, M., Aoki, M., Miyoshi, I., Kato, M., Pasinelli, P., Kasai, N., Brown, R. H., Jr., and Itoyama, Y. (2001) *J. Neurosci.* **21,** 9246–9254
14. Nakagawara, A. (1998) *Med. Pediatr. Oncol.* **31,** 113–115
15. Harvey, K. F., and Kumar, S. (1999) *Trends Cell Biol.* **9,** 166–169
16. Kumar, S., Tomooka, Y., and Noda, M. (1992) *Biochem. Biophys. Res. Commun.* **30,** 1155–1161
17. Kato, S., Takikawa, M., Nakashima, K., Hirano, A., Cleveland, D. W., Kusaka, H., Shibata, N., Kato, M., Nakano, I., and Ohama, E. (2000) *Amyotroph. Lateral Scler. Other Motor Neuron Disord.* **1,** 163–184
18. Orrell, R. W. (2000) *Neuromuscul. Disord.* **10,** 63–68
19. Cudkowicz, M. E., McKenna-Yasek, D., Sapp, P. E., Chin, W., Geller, B., Hayden, D. L., Schoenfeld, D. A., Hosler, B. A., Horvitz, H. R., and Brown, R. H., Jr. (1997) *Ann. Neurol.* **41,** 210–221
20. Ratovitski, T., Corson, L. B., Strain, J., Wong, P., Cleveland, D. W., Culotta, V. C., and Borchelt, D. R. (1999) *Hum. Mol. Genet.* **8,** 1451–1460
21. Aoki, M., Ogasawara, M., Matsubara, Y., Narisawa, K., Nakamura, S., Itoyama, Y., and Abe, K. (1993) *Nat. Genet.* **5,** 323–324
22. Kato, M., Aoki, M., Ohta, M., Nagai, M., Ishizaki, F., Nakamura, S., and Itoyama, Y. (2001) *Neurosci. Lett.* **312,** 165–168
23. Andersen, P. M., Forsgren, L., Binzer, M., Nilsson, P., Ala-Hurula, V., Keranen, M. L., Bergmark, L., Saarinen, A., Haltia, T., Tarvainen, I., Kinnunen, E., Udd, B., and Marklund, S. L. (1996) *Brain* **119,** 1153–1172
24. Shibata, N., Hirano, A., Kobayashi, M., Siddique, T., Deng, H. X., Hung, W.-Y., Kato, T., and Asayama, K. (1996) *J. Neuropathol. Exp. Neurol.* **55,** 481–490
25. Sussman, D. J., Klingensmith, J., Salinas, P., Adams, P. S., Nusse, R., and Perrimon, N. (1994) *Dev. Biol.* **166,** 73–86
26. Wodarz, A., and Nusse, R. (1998) *Annu. Rev. Cell Dev. Biol.* **14,** 59–88
27. Boutros, M., Paricio, N., Strutt, D. I., and Mlodzik, M. (1998) *Cell* **94,** 109–118
28. Julien, J. P. (2001) *Cell* **104,** 581–591
29. Fons, R. D., Bogert, B. A., and Hegde, R. S. (2003) *J. Cell Biol.* **160,** 529–539
30. Fujita, Y., Okamoto, K., Sakurai, A., Gonatas, N. K., and Hirano, A. (2000) *J. Neurol. Sci.* **174,** 137–140
31. Mourelatos, Z., Gonatas, N. K., Stieber, A., Gurney, M. E., and Dal Canto, M. C. (1996) *Proc. Natl. Acad. Sci. U. S. A.* **93,** 5472–5477
32. Wharton, K. A., Jr. (2003) *Dev. Biol.* **253,** 1–17
33. Tsang, M., Lijam, N., Yang, Y., Beier, D. R., Wynshaw-Boris, A., and Sussman, D. J. (1996) *Dev. Dyn.* **207,** 253–262
34. Krylova, O., Messenger, M. J., and Salinas, P. C. (2000) *J. Cell Biol.* **151,** 83–94
35. Julien, J. P., and Beaulieu, J. M. (2000) *J. Neurol. Sci.* **180,** 7–14
36. Luo, Z. G., Wang, Q., Zhou, J. Z., Wang, J., Luo, Z., Liu, M., He, X., Wynshaw-Boris, A., Xiong, W. C., Lu, B., and Mei, L. (2002) *Neuron* **35,** 489–505
37. De Ferrari, G. V., and Inestrosa, N. C. (2000) *Brain Res. Brain Res. Rev.* **33,** 1–12
38. Kaytor, M. D., and Orr, H. T. (2000) *Curr. Opin. Neurobiol.* **12,** 275–278
39. Versteeg, R., Caron, H., Cheng, N. C., van der Drift, P., Slater, R., Westerveld, A., Voute, P. A., Delattre, O., Laureys, G., van Roy, N., and Speleman, F. (1995) *Eur. J. Cancer* **31,** 538–541
40. Murata, S., Minami, Y., Minami, M., Chiba, T., and Tanaka, K. (2001) *EMBO Rep.* **2,** 1133–1138
41. Okado-Matsumoto, A., and Fridovich, I. (2002) *Proc. Natl. Acad. Sci. U. S. A.* **99,** 9010–9014
42. Niwa, J., Ishigaki, S., Hishikawa, N., Yamamoto, M., Doyu, M., Murata, S., Tanaka, K., Taniguchi, N., and Sobue, G. (2002) *J. Biol. Chem.* **277,** 36793–36798
43. Mori, K. (2000) *Cell* **101,** 451–454
44. Travers, K. J., Patil, C. K., Wodicka, L., Lockhart, D. J., Weissman, J. S., and Walter, P. (2000) *Cell* **101,** 249–258
45. Wickner, S., Maurizi, M. R., and Gottesman, S. (1999) *Science* **286,** 1888–1893
46. Borchelt, D. R., Lee, M. K., Slunt, H. S., Guarnieri, M., Xu, Z. S., Wong, P. C., Brown, R. H., Jr., Price, D. L., Sisodia, S. S., and Cleveland, D. W. (1994) *Proc. Natl. Acad. Sci. U. S. A.* **16,** 8292–8296

Acta Neuropathol (2004) 107 : 149–158
DOI 10.1007/s00401-003-0791-1

REGULAR PAPER

Shinsuke Kato · Yusuke Saeki · Masashi Aoki · Makiko Nagai · Aya Ishigaki · Yasuto Itoyama · Masako Kato
Kohtaro Asayama · Akira Awaya · Asao Hirano · Eisaku Ohama

Histological evidence of redox system breakdown caused by superoxide dismutase 1 (SOD1) aggregation is common to SOD1-mutated motor neurons in humans and animal models

Received: 8 July 2003 / Revised: 10 October 2003 / Accepted: 13 October 2003 / Published online: 27 November 2003

Abstract Living cells produce reactive oxygen species (ROSs). To protect themselves from these ROSs, the cells have developed both an antioxidant system containing superoxide dismutase 1 (SOD1) and a redox system including peroxiredoxin2 (Prx2, thioredoxin peroxidase) and glutathione peroxidase1 (GPx1): SOD1 converts superoxide radicals into hydrogen peroxide (H_2O_2), and H_2O_2 is then converted into harmless water (H_2O) and oxygen (O_2) by Prx2 and GPx1 that directly regulate the redox system. To clarify the biological significance of the interaction of the redox system (Prx2/GPx1) with SOD1 in SOD1-mutated motor neurons in vivo, we produced an affinity-purified rabbit antibody against Prx2 and investigated the immunohistochemical localization of Prx2 and GPx1 in neuronal Lewy body-like hyaline inclusions (LBHIs) in the spinal cords of familial amyotrophic lateral sclerosis (FALS) patients with a two-base pair deletion at codon 126 and an Ala→Val substitution at codon 4 in the SOD1 gene, as well as in transgenic rats expressing human SOD1 with H46R and G93A mutations. The LBHIs in motor neurons from the SOD1-mutated FALS patients and transgenic rats showed identical immunoreactivities for Prx2 and GPx1: the reaction product deposits with the antibodies against Prx2 and GPx1 were localized in the LBHIs. In addition, the localizations of the immunoreactivities for SOD1 and Prx2/GPx1 were similar in the inclusions: the co-aggregation of Prx2/GPx1 with SOD1 in neuronal LBHIs in mutant SOD1-related FALS patients and transgenic rats was evident. Based on the fact that Prx2/GPx1 directly regulates the redox system, such co-aggregation of Prx2/GPx1 with SOD1 in neuronal LBHIs may lead to the breakdown of the redox system itself, thereby amplifying the mutant SOD1-mediated toxicity in mutant SOD1-linked FALS patients and transgenic rats expressing human mutant SOD1.

Keywords Peroxiredoxin 2 · Glutathione peroxidase 1 · Redox system · Superoxide dismutase 1 · Familial amyotrophic lateral sclerosis

S. Kato (✉) · Y. Saeki · E. Ohama
Department of Neuropathology,
Institute of Neurological Sciences, Faculty of Medicine,
Tottori University,
Nishi-cho 36-1, 683-8504 Yonago, Japan
Tel.: +81-859-348034, Fax: +81-859-348289,
e-mail: kato@grape.med.tottori-u.ac.jp

M. Aoki · M. Nagai · A. Ishigaki · Y. Itoyama
Department of Neuroscience, Division of Neurology,
Tohoku University Graduate School of Medicine, Sendai, Japan

M. Kato
Division of Pathology, Tottori University Hospital,
Yonago, Japan

K. Asayama
Department of Pediatrics,
University of Occupational and Environmental Health,
Kitakyushu, Japan

A. Awaya
Japan Science and Technology Corporation,
Tachikawa, Japan

A. Hirano
Division of Neuropathology,
Department of Pathology, Montefiore Medical Center,
Bronx, New York, USA

Introduction

Living cells produce reactive oxygen species (ROSs) during physiological processes and in response to external stimuli such as ultraviolet radiation. To protect itself from potentially destructive ROSs, each cell of living organisms has developed a sophisticated antioxidant enzyme defense system. In this system, there are two groups of enzymes: the enzymes of the first group convert superoxide radicals into hydrogen peroxide (H_2O_2), and the enzymes of the second group convert H_2O_2 into harmless water (H_2O) and oxygen (O_2). For the first antioxidant enzyme group, three isoforms of superoxide dismutase (SOD) [EC 1.15.1.1] have been identified: SOD1, SOD2, and SOD3 [9]. In the second enzyme group, the peroxiredoxin (Prx) and glutathione peroxidase (GPx) families, as well as catalase localized within peroxisomes have been identified. Unlike

SOD and catalase, enzymes of the Prx and GPx families require secondary enzymes and cofactors to function at high efficiency. In particular, the enzymes of the Prx- and GPx-families are considered to play a role in directly controlling the redox system. In general, the redox system regulates versatile control mechanisms in signal transduction and gene expression [29]. In mammalian cells, this redox signal transduction is linked to systems such as cellular differentiation, immune response, growth control, and apoptosis [10].

Peroxiredoxin2 (Prx2) is a novel organ-specific antioxidative enzyme that is mainly expressed in mammalian brain [23]. This protein is a member of Prx family, whose members possess reactive cysteine residues [23]. Prx2 requires thioredoxin reductase (TR) as a secondary enzyme as well as thioredoxin and NADPH as cofactors to function at high efficiency; the activity of Prx2 in the thioredoxin/TR/NADPH system is over five times higher than that of Prx2 by itself [5]. In this milieu, Prx2 is also called thioredoxin peroxidase 1 (thioredoxin-dependent peroxide reductase 1) or thiol-specific antioxidant [4, 5, 6]. In addition to controlling the intracellular content of H_2O_2, Prx2 directly regulates the redox signals of the thioredoxin/TR/NADPH system, because alone the secondary enzyme and cofactors (i.e., thioredoxin/TR/NADPH) can not directly regulate the redox system and can not act on H_2O_2. Cytosolic GPx [EC 1.11.1.9], a classical selenium-dependent isoform (also assigned as GPx1), was first described as an enzyme that protects hemoglobin from oxidative degradation in red blood cells [25]. The GPx family is composed of at least four GPx isoforms in mammals [7]. Among them, GPx1 is considered as the major enzyme responsible for removing intracytoplasmic H_2O_2. Like Prx2, GPx1 needs glutathione reductase (GR) as a secondary enzyme as well as glutathione and NADPH as cofactors to work at high efficiency, and this process is also one of the redox signals in living cells [21, 24]. Therefore, Prx2 and GPx1 directly control the redox system.

Approximately 20% of the cases of familial amyotrophic lateral sclerosis (FALS) are caused by a mutant SOD1 [15, 17, 18]. SOD1 is thought to be an essential component of neuronal Lewy body-like hyaline inclusions (LBHIs): neuronal LBHIs in affected anterior horn cells are morphological hallmarks of SOD1-mutated motor neurons of FALS patients [3, 11, 12, 13, 14, 15, 16, 17, 18, 30]. To cope with destructive ROSs, even SOD1-mutated motor neurons induce mutant and wild-type SOD1 as well as Prx2 and GPx1. Considering that Prx2 and GPx1 interact not only with wild-type SOD1 but also with mutant SOD1, the interaction of Prx2/GPx1 with SOD1 has been suggested to contribute to mutant SOD1 aggregation toxicity: Prx2/GPx1 possibly aggregate as LBHIs in SOD1-mutated motor neurons. Furthermore, the aggregation of Prx2/GPx1 might affect the intracytoplasmic redox regulation and amplify mutant SOD1-mediated toxicity. To clarify the biological significance of the interaction of Prx2/GPx1 (redox system) with SOD1 in SOD1-mutated motor neurons in vivo, we first produced an antibody against Prx2, and analyzed the characteristic expressions of both Prx2 and GPx1 in neuronal LBHIs in SOD1-mutated motor neurons of humans and animal models.

Materials and methods

Preparation of polyclonal antibody against Prx2

A synthetic peptide corresponding to the C-terminal region of Prx2 (amino acids 184–198: NH_2-KPNVDDSKEYFSKHN-COOH) with or without conjugation to human serum albumin (HSA) at the carboxyl end was supplied by Peptide Institute (Osaka, Japan). This amino acid sequence is homologous with those of the C-terminal region of the human, rat or mouse Prx2. The polyclonal antibody preparation was carried out according to the method of Kato et al. [16]. To prepare immunogen, 6 mg synthesized Prx2 peptide was conjugated with 6 mg keyhole limpet hemocyanin (KLH) in the presence of 50 mM 1-ethyl-3-(3-dimethylaminopropyl) carbodiimide-HCl (Pierce Chemical Co., Rockford, IL) and 2.5 mM *N*-hydroxysulfosuccinimide (Pierce) in 3 ml phosphate-buffered saline (PBS) pH 7.4 for 1 h at room temperature. The reaction was terminated by adding 2-mercaptoethanol to the concentration of 20 mM and dialyzed against PBS for 24 h. To raise polyclonal antibodies, 500 µg of the immunogen in 50% Freund's complete adjuvant was inoculated intradermally into a rabbit at 20 skin sites; four booster inoculations of 500 µg immunogen in 50% Freund's incomplete adjuvant were given at 10, 17, 24 and 31 days after the first inoculation. The serum was taken 10 days after the final immunization. The IgG fraction in the antiserum against the immunogen, the hapten-conjugated KLH, was purified by absorption on a protein G-Sepharose gel column (Pharmacia Biotech, Uppsala, Sweden). Subsequently, the antibodies were further purified on an affinity column of immobilized KLH conjugated with the synthetic Prx2 peptide, as described previously [16].

Enzyme-linked immunosorbent assay

Noncompetitive ELISA was carried out according to the method described by Kato et al. [16]. Each well of a 96-well microtiter plate was coated with 100 µl of 5 µg/ml immunogen in 5 mM sodium carbonate buffer (pH 9.6) and incubated for 60 min. This was followed by triplicate washing with PBS containing 0.05% Tween 20 (buffer A). Each well was blocked with 0.5% gelatin for 60 min and then washed three times with buffer A. Antibody solutions (100 µl) at the concentrations indicated in Fig. 1 (horizontal line) were added to each well and incubated for 60 min. The wells were then washed three times with buffer A. The binding of the horseradish peroxidase-conjugated secondary antibody (Wako Pure Chemical Industries, Osaka, Japan) to the primary antibody was visualized with 2, 2'-azino-bis-(3-ethylbenzothiazoline-6-sulfonate)-$(NH_3)_2$. The reaction was terminated with 1 M sulfuric acid, and the absorbance at 415 nm was read on a micro-ELISA plate reader (Tecan, Hombrechtikon, Switzerland).

Tissue collection

Histochemical and immunohistochemical studies were performed on archival, buffered 10% formalin-fixed, paraffin-embedded tissues obtained at autopsy from five FALS patients who were members of two different families. The main clinicopathological characteristics of the FALS patients are summarized in Table 1, and have been reported previously [12, 13, 20, 22, 28, 30, 31]. SOD1 analysis revealed that the members of the Japanese Oki family had a two-base pair deletion at codon 126 (frame-shift 126 mutation) [12] and the American C family members had an Ala→Val substitution at codon 4 (A4V) [30]. As human controls, we examined autopsy specimens of the spinal cord from 20 neurologically and neuropathologically normal individuals (11 male, 9 females; aged 37–75 years).

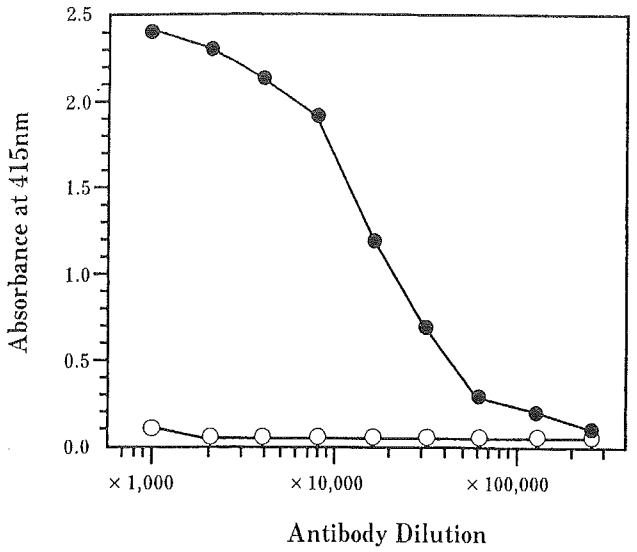

Fig. 1 Specificity of antibody against Prx2. The immunoreactivity of the antibody to HSA-conjugated Prx2 peptide (*solid circles*) and native HSA (*open circles*) was determined by noncompetitive ELISA. The anti-Prx2 antibody recognizes the HSA-conjugated Prx2 peptide, but does not react with HAS (*Prx2* peroxiredoxin2, *ELISA* enzyme-linked immunosorbent assay, *HAS* human serum albumin)

Histochemical and immunohistochemical studies were also carried out on specimens from transgenic rats with the H46R and G93A types of mutations (three rats of each type). The H46R rats used in this study were a transgenic line (H46R-4) in which the level of human SOD1 with the H46R mutation was 6 times the level of that of endogenous rat SOD1 [27]. The G93A rats were a transgenic line (G93A-39) in which the level of human SOD1 with the G93A mutation was 2.5 times the level of endogenous rat SOD1 [27]. These rats were killed at an age of over 180 days; an age corresponding to an advanced stage of disease in these strains. The detailed clinical signs and pathological characteristics of the neuronal LBHIs of the H46R and G93A rats have been demonstrated previously [27]. As rat controls, we investigated the spinal cord specimens of three age-matched littermates of H46R and G93A rats and five age-matched normal Sprague-Dawley rats. Rats were anesthetized with sodium pentobarbital (0.1 ml/100 g body weight). After perfusion of the rats via the aorta with physiological saline at 37°C, they were fixed by perfusion with 4% paraformaldehyde in 0.1 M cacodylate buffer (pH 7.3). The spinal cords were removed and then postfixed in the same solution.

Histochemistry and immunohistochemistry

After fixation, the specimens were embedded in paraffin, cut into 6-μm-thick sections, and examined by light microscopy. Spinal cord sections were stained by the following histochemical methods: hematoxylin and eosin (HE), Klüver-Barrera, Holzer, phosphotungstic acid-hematoxylin, periodic acid-Schiff, alcian blue, Masson's trichrome, Mallory azan and Gallyas-Braak stains. Representative paraffin sections were used for immunohistochemical assays. The following primary antibodies were utilized: an affinity-purified rabbit antibody against Prx2 (concentration: 1 μg/ml), a polyclonal antibody to GPx1 [diluted 1:2,000 in 1% bovine serum albumin-containing phosphate-buffered saline (BSA-PBS), pH 7.4] [2], and a polyclonal antibody to human SOD1 (diluted 1:10,000 in 1% BSA-PBS, pH 7.4) [1]. Sections were deparaffinized, and endogenous peroxidase activity was quenched by incubation for 30 min with 0.3% H_2O_2. The sections were then washed in PBS. Normal sera homologous with secondary antibody was used as a blocking reagent. Tissue sections were incubated with the primary antibodies for 18 h at 4°C. PBS-exposed sections served as controls. As a preabsorption test, some sections were incubated with the anti-Prx2 antibody that had been preabsorbed with an excess amount of the synthetic Prx2 peptide. Bound antibodies were visualized by the avidin-biotin-immunoperoxidase complex (ABC) method using the appropriate Vectastain ABC Kit (Vector Laboratories, Burlingame, CA) and 3,3'-diaminobenzidine tetrahydrochloride (DAB; Dako, Glostrup, Denmark) as chromogen.

Results

We successfully produced an affinity-purified rabbit antibody against Prx2 peptide (amino acids 184–198; although this amino acid sequence is homologous with that of each C-terminal region of the human, rat, mouse, Chinese hamster or Bos Taurus Prx2, this peptide does not share homology with other members of the Prx family or any other peptide sequence in GenomeNet), and applied it to stain of paraffin sections from both humans and rats. This anti-Prx2 antibody recognized the HSA-conjugated Prx2 peptide, but did not react with HSA (Fig. 1).

Analysis of the essential changes of five cases of FALS revealed a subtype of FALS with posterior column involvement (PCI). This subtype is characterized by the degeneration of the middle root zones of the posterior column, Clarke nuclei, and the posterior spinocerebellar tracts, in addition to spinal cord motor neuron lesions. A long-term surviving patient with a clinical course of 11 years

Table 1 Characteristics of five FALS cases (*FALS* familial amyotrophic lateral sclerosis, *SOD* superoxide dismutase, *LBHI* Lewy body-like hyaline inclusion, *2-bp* two-base pair, *PCI* posterior column involvement type, + detected, *ND* not determined, *As* asphyxia, *IH* intraperitoneal hemorrhage, *RD* respiratory distress, *Pn* pneumonia)

Case	Age (years)	Sex	Cause of Death	FALS Duration	SOD1 mutation	FALS subtype	Neuronal LBHI
Japanese Oki family							
1	46	F	As	18 months	2-bp deletion (126)	PCI	+
2	65	M	IH	11 years	2-bp deletion (126)	PCI and degeneration of other systems	+
American C family							
3	39	M	RD	7 months	A4V	PCI	+
4	46	M	Pn	8 months	A4V	PCI	+
5	66	M	Pn	1 year	ND	PCI	+

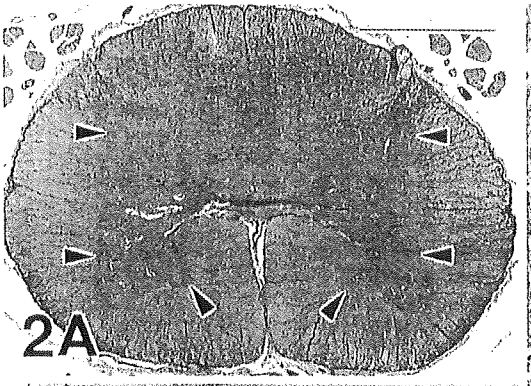
2A

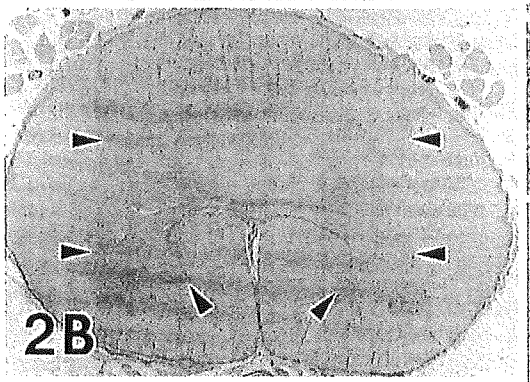
2B

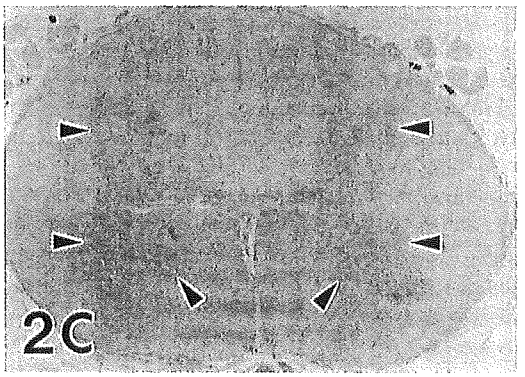
2C


3A


3C

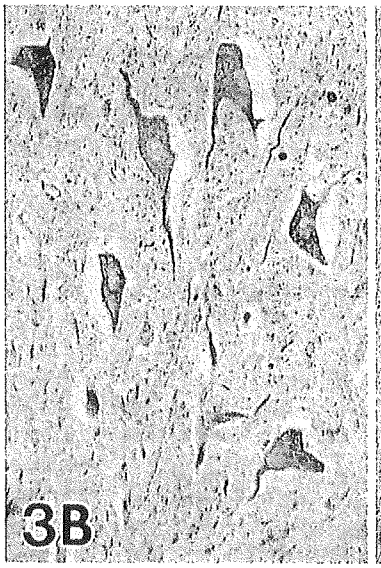
3B

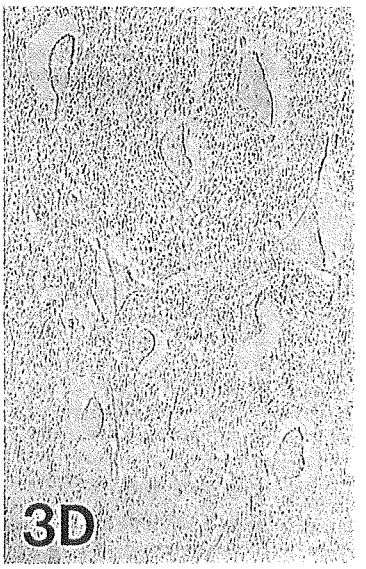
3D

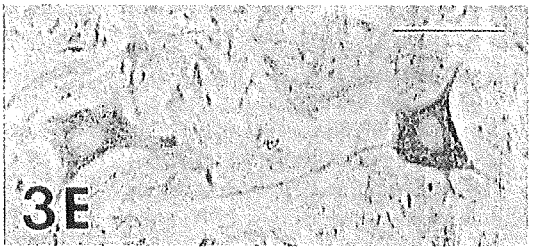
3E

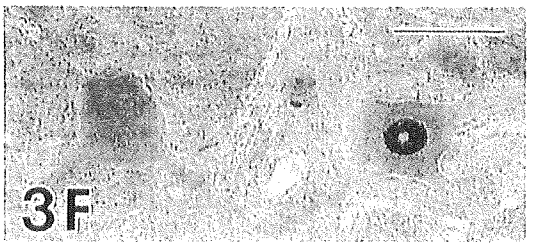
3F

◀ **Fig. 2** Serial transverse sections through the lumbar segments of the normal human spinal cords. **A** Light microscopic preparation stained with HE. **B, C** Immunostaining for GPx1 (**B**) and Prx2 (**C**). GPx1 and Prx2 immunoreactivities are found diffusely in the neuropil with considerably less intensity (*arrowheads*). No counterstaining (*HE* hematoxylin and eosin, *GPx1* glutathione peroxidase1, *Prx2* peroxiredoxin2). *Bar* **A** (also for **B, C**) 2 mm

Fig. 3 Detection of Prx2 and GPx1 in the normal motor neurons of the human spinal cord. **A–D** Serial sections. **A** Staining with HE. **B** Immunostaining with the antibody against GPx1, showing GPx1-positive neurons. **C** Immunostaining with the antibody to Prx2. Immunoreactivity is identified in most of the neurons. Thus, most of the normal motor neurons in the spinal cord co-express both GPx1 (**B**) and Prx2 (**C**), although their staining intensities in neurons vary. **D** Immunostaining with anti-Prx2 antibody pretreated with an excess of the synthetic Prx2 peptide. No immunoreaction products are observed in the motor neurons and neuropil. **E** GPx1 immunostaining of the neuronal cytoplasm and proximal dendrites is observed, but no intranuclear localization is seen. **F** Prx2 immunostaining of the neuronal cytoplasm and proximal dendrites is observed, and a nucleus of the neuron is also immunostained by the anti-Prx2 antibody. **B–F** No counterstaining (*HE* hematoxylin and eosin, *GPx1* glutathione peroxidase1, *Prx2* peroxiredoxin2). *Bars* **A** (also for **B–D**) 100 μm; **E, F** 50 μm

(case 2 in Table 1) showed multisystem degeneration in addition to the features of FALS with PCI. Neuronal Lewy body-like hyaline inclusions (LBHIs) were present in all five FALS cases. As observed in HE preparations, the neuronal LBHIs in the FALS patients were essentially identical to those in the H46R and G93A transgenic rats; the inclusions were round eosinophilic or paler inclusions and often showed eosinophilic cores with pale peripheral halos. In mutant SOD1-linked FALS patients, the neuronal LBHIs were generally composed of eosinophilic cores with pale peripheral halos and sometimes showed ill-defined forms that consisted of obscure eosinophilic materials. In H46R and G93A transgenic rats, the intracytoplasmic LBHIs with cores and halos were less frequently observed and round or sausage-like LBHIs, which were though to be intradendritic LBHIs, were often seen in the neuropil, although these round or sausage-like LBHIs in the neuropil were not remarkable in the human FALS patients. Histochemically, most of the neuronal LBHIs in the H46R and G93A transgenic rats were argyrophilic in Gallyas-Braak stain, and they were generally blue to violet after Masson's trichrome or Mallory azan staining, similar to the histochemical findings of the neuronal LBHIs of the human FALS patients. The spinal cords of normal individuals in both humans and rats did not exhibit any distinct histopathological alterations.

When control and representative paraffin sections were incubated with PBS alone (i.e., no primary antibody), no staining was detected. Prx2 immunoreactivity in normal spinal cords was identified in almost all neurons. In addition, Prx2-immunostaining was found throughout the neuropil with considerably lower intensity (Fig. 2A, C). With respect to the intracellular localization of Prx2, immunostaining of the neuronal cytoplasm and proximal dendrites was specifically observed (Fig. 3A, C). Additionally, the nuclei of some neurons were immunostained by the anti-Prx2 antibody, albeit the staining of positively stained nuclei varied (Fig. 3F). Incubation of sections with anti-Prx2 antibody that had been pretreated with an excess of the synthetic Prx2 produced no staining (Fig. 3D).

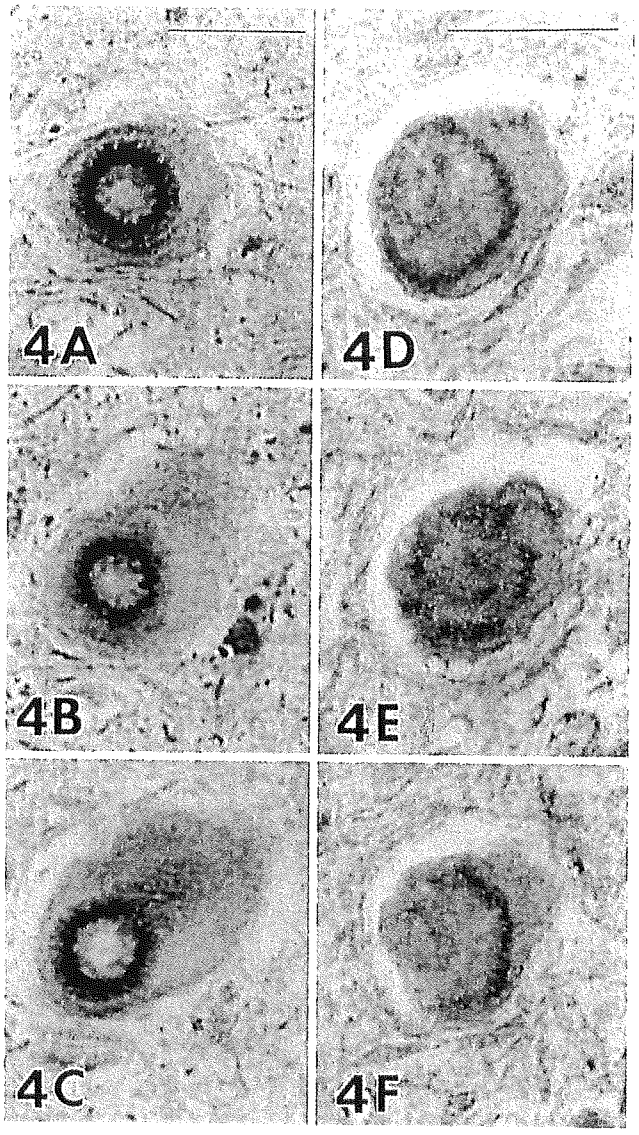

Fig. 4A–C Serial sections of a typical LBHI with a core and halo in neurons from the spinal cord of an FALS patient with a two-base pair deletion in the SOD1 gene. **A** Immunostaining for SOD1: immunoreactivity is mostly restricted to the halo. **B** Immunostaining for GPx1: immunoreactivity is located in the SOD1-positive portion of the LBHI. **C** Immunoreactivity for Prx2. Co-localization of the three proteins SOD1, GPx1 and Prx2 in the LBHI is evident. **D–F** Serial sections of a core and halo-type LBHI in a transgenic rat expressing human SOD1 with an H46R mutation. Immunostaining for SOD1 (**D**), GPx1 (**E**) and Prx2 (**F**). Similar stainability and immunolocalization of SOD1, GPx1 and Prx2 in the LBHI are observed (*LBHI* Lewy body-like hyaline inclusion, *FALS* familial amyotrophic lateral sclerosis, *SOD1* superoxide dismutase 1, *GPx1* glutathione peroxidase1, *Prx2* peroxiredoxin2). **A–F** No counterstaining. *Bars* **A** (also for **B, C**), **D** (also for **E, F**) 25 μm

A neuropil staining pattern similar to that for Prx2 was observed with GPx1; weak GPx1 immunoreactivity was diffusely seen in the neuropil in transverse sections of the

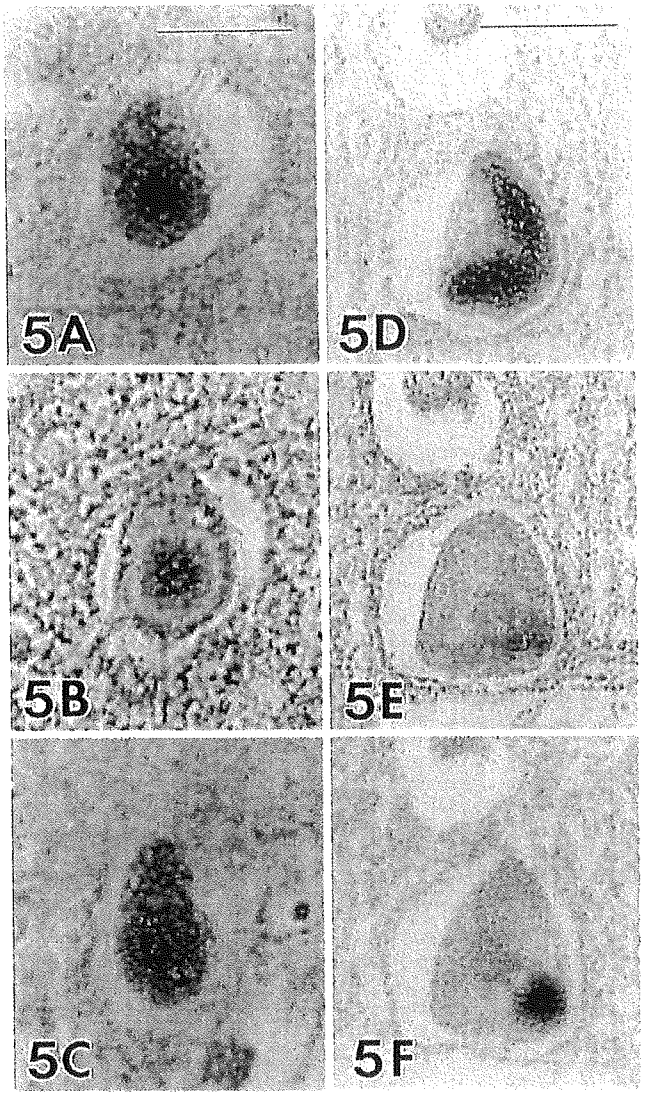

Fig. 5A–C Serial sections of an LBHI in an FALS patient with an A4V mutation in SOD1 gene. Immunostaining for SOD1 (**A**), GPx1 (**B**) and Prx2 (**C**). Co-localization of the three proteins in the LBHI is mainly observed in the core (**A–C**). **D–F** Serial sections of an LBHI in an FALS patient with a two-base pair deletion in the SOD1 gene. Immunostaining for SOD1 (**D**), GPx1 (**E**) and Prx2 (**F**). Immunostaining GPx1 (**E**) and Prx2 (**F**) are observed in only part of the SOD1-positive LBHI. The precise intra-inclusional immunolocalizations of these three proteins differ from each other in this LBHI (*LBHI* Lewy body-like hyaline inclusion, *FALS* familial amyotrophic lateral sclerosis, *SOD1* superoxide dismutase 1, *GPx1* glutathione peroxidase1, *Prx2* peroxiredoxin2). *Bars* **A** (also for **B**, **C**), **D** (also for **E**, **F**) 25 μm

spinal cords (Fig. 2A, B). GPx1 immunostaining was observed in the cytoplasm with cell bodies and proximal dendrites being essentially identified (Fig. 3A, B, E), but no intranuclear staining was observed (Fig. 3B, E). The stainability and intensity of Prx2 and GPx1 in the normal anterior horn cells of the spinal cords in humans were identical to those in rats. Therefore, almost all of the normal motor neurons in the spinal cords co-expressed both Prx2 and GPx1 (Fig. 3A–C), although the staining intensities of positively stained neurons varied.

Corroborating recent findings [12, 13, 16, 19, 27, 30], almost all of the neuronal LBHIs in both the FALS patients from two different families and races (Japanese Oki family and American C family) and the transgenic rats expressing two different human SOD1 mutations (H46R and G93A) were intensely immunostained by the antibody against human SOD1 (Figs. 4A, D; 5A, D; 6A; 7A). Most neuronal LBHIs were also immunoreactive for Prx2, although the intensity of Prx2 immunoreactivity in the LBHIs varied (Figs. 4C, F; 5C, F; 6B). The LBHIs in the neurons of the FALS patients and transgenic rats (H46R and G93A) showed a similar immunoreactivity for Prx2. The Prx2 immunolocalization in many intracytoplasmic and intraneuritic LBHIs was similar to that of SOD1 in both diseases. In core and halo-type LBHIs, the reaction product deposits of the antibody against Prx2 were generally restricted to the periphery (Fig. 4C, F), and were sometimes localized in the cores alone (Fig. 5C). In ill-defined LBHIs, Prx2 immunostaining was distributed throughout each inclusion. In some inclusions, however, expression of Prx2 was observed in only part of the inclusion (Fig. 5F). With respect to the GPx1 immunostaining in the neuronal LBHIs, similar stainability and immunolocalization to Prx2 were confirmed in the core and halo types as well as the ill-defined forms; most LBHIs in neurons were immunostained by the anti-GPx1 antibody with various intensities (Figs. 4B, E; 5B, E; 7B). The immunoreactivity for GPx1 in the FALS patients was similar to that in the transgenic rats (H46R and G93A). Like Prx2, the immunolocalization of GPx1 was similar to that of SOD1 in both diseases. GPx1-immunoreactive products in many core and halo-type inclusions were mainly localized in the periphery portions (Fig. 4B, E), but sometimes in the core portions alone (Fig. 5B). In some inclusions, the reaction products were confined to certain regions of each inclusion (Fig. 5E).

Noticeably, the co-localization of the three proteins SOD1, Prx2 and GPx1 in neuronal LBHIs in SOD1-mutated FALS patients and transgenic rats (H46R and G93A) was evident (Figs. 4, 5, 6, 7), although all three immunoreactive intensities varied. With respect to the intra-inclusional localization, many inclusions showed similar co-localizations of these three proteins (Figs. 4, 5A–C). In some LBHIs, the precise intra-inclusional immunolocalizations of the three proteins differed: Prx2 (Fig. 5D, F) and GPx1 (Fig. 5D, E) immunostaining was observed in only some areas of the SOD1-positive LBHIs.

Discussion

Under normal physiological conditions, Prx2 and GPx1 immunoreactivities in the spinal cord anterior horns in humans and rats are primarily identified in the neurons: cytoplasmic staining with both antibodies is observed in almost all of the anterior horn cells. Like Prx1 [26, 33], intranuclear localization in some neurons is also observed in Prx2 immunostaining. Considering that endogenous Prx2